Development of Freshwater Hazard Indicators to Assess Climate Change Impacts to Salmon

November 25, 2024

Markus Schnorbus, Arelia Schoeneberg, Travis Tai, Samah Larabi, and Lee Zeman

Pacific Climate Impacts Consortium

University of Victoria

Citation

Schnorbus, M.A, A. Schoeneberg, T. Tai, S. Larabi, and L. Zeeman, 2024: *Development of Freshwater Hazard Indicators to Assess Climate Change Impacts to Salmon*. Pacific Climate Impacts Consortium, University of Victoria, Victoria, BC, 60 pp.

About PCIC

The Pacific Climate Impacts Consortium (PCIC) is a regional climate service centre at the University of Victoria that provides practical information on the physical impacts of climate variability and change in the Pacific and Yukon Region of Canada. We collaborate with climate researchers and regional stakeholders to produce knowledge and tools in support of long-term planning. For more information see http://www.pacificclimate.org/.

Disclaimer

Acknowledgement

We gratefully acknowledge the financial support from the British Columbia Salmon Restoration and Innovation Fund (BCSRIF), which is co-funded by the federal Department of Fisheries and Oceans (DFO) and the Province of British Columbia. We would also like to thank Howard Stiff and Sue Grant of the Department of Fisheries and Oceans for their generous time and effort spent in discussion, and for providing thoughtful guidance and direction to this project. The work represented in this report also benefitted from the efforts of PCIC employees, both past and present, who contributed technical expertise to the project, including Nigus Demelash Melaku, Md. Shahabul Alam, Ameneh Mollasharifi Targhi, Rod Glover, and James Hiebert.

Finally, a special acknowledgement goes to the late Kim Hyatt. Kim was the inspiration and driving force behind this project, and none of what has been accomplished would have been possible without his passion for salmon conservation and management.

Table of Contents

List of Figures

List of Tables

1 Introduction

1.1 Background

A number of key Pacific salmon stocks have declined in recent years (WSAC, 2019). While these declines have been attributed to a variety of causes (Dorner et al., 2017; Fisheries and Oceans Canada, 2016; Peterman and Dorner, 2012), the impacts of climate change on freshwater systems are undoubtedly significant contributing factors, along with other impacts from human activities. The limited body of existing area-specific research in Canada's Pacific region highlights a range of either observed or potential future impacts of climate change, in particular, on salmon populations in British Columbia (Battin et al., 2007; Hinch and Martins, 2011; Hyatt et al., 2003; Hyatt et al., 2015; Isaak et al., 2012). Most of this research is focused on only a few locations and salmon populations (Stiff et al., 2018b), with most of the effort dedicated to Sockeye Salmon in the Fraser River main-stem (Crossin et al., 2008; Healey, 2011; Macdonald et al., 2012; Martins et al., 2011; Morrison and Foreman, 2005). Consequently, we do not yet have a comprehensive understanding of potential threats to Pacific salmonids and their biodiversity due to climate change.

The changing climate in BC is expected to affect various hydrological factors (flow levels, timing, and water temperature) pertinent to salmon growth, survival, and habitat interconnectivity, leading to changes in species distribution at broad spatial scales (Isaak et al., 2012; Wade et al., 2013). While these studies suggest that change will occur as the climate continues to warm, more detailed information is required to support actions to protect wild salmon and associated habitat. Mitigating the threats to salmonids requires action to protect genetic diversity to ensure the greatest potential for adaptation to changing climatic conditions. To be effective, such efforts need to be supported by a concerted effort to bridge the significant knowledge gaps that remain due to the uneven geographic coverage and associated uncertainty regarding the nature and magnitude of regional impacts of climate change on hydrology, geomorphology, seasonal thermal regimes, and salmon biology in many British Columbia watersheds.

It is therefore necessary to understand how salmonid habitats may be affected by ongoing and future effects of climate change at regional and watershed-scales. For example, failure to understand how climate change will influence wild salmon production in various regions will contribute to controversies in which the effects of fishing or local scale aquaculture continue to be blamed for all changes. Poorly informed restoration activities for salmon watersheds that are likely to be highly vulnerable to climate impacts projected to occur within 25-50 years may not further the goal of sustainable salmon restoration (e.g. Battin et al., 2007).

The goal of this project is to provide the data, results and tools required to enable the development and implementation of watershed and population specific science-based ecological vulnerability assessments in support of wild salmon conservation and protection. This will be achieved via improved understanding of the effect of climate change and variability on the terrestrial freshwater environments in which salmon populations are found. The proposed product is a quantification of freshwater hazard for salmon populations throughout the Pacific Region delivered to a broad range of users via an online tool, the Salmon Climate Impacts Portal. This improved knowledge and accompanying tool will expand the scope of current understanding, which is based on a limited number of sites and species, to a much larger domain covering a broad range of climatic and bio-geographic zones, all six salmon species, and many salmon conservation units.

1.2 Scope and Deliverables

Fisheries management must address the effects of climate change across a diversity of species and aquatic environments (Hunter et al., 2015). However, climate risk is a complex process that requires understanding of the variability in climate change vulnerability between species, populations, and habitats. Climate change risk, or vulnerability, assessments are important tools to aid in the adaptation process, raise awareness, and advance scientific understanding (IPCC, 2014). Vulnerability assessments can be used to explore the spatial variability of climate risk and can be used to identify and prioritize at-risk salmon populations (FAO, 2015; Hunter et al., 2015). In this context vulnerability assessment can provide a relative comparison across salmon species and populations to highlight populations that, depending upon management priorities, are high priorities for conservation and/or recovery efforts.

Ecological vulnerability is described as the degree to which a system or species is susceptible to, or unable to cope with, effects of climate change, including variability and extremes (Hunter et al., 2015). Quantifying the vulnerability of salmon to future climate change typically follows the framework outlined by the IPCC wherein ecological vulnerability is determined by interaction between the occurrence of a hazard, and the sensitivity to the hazard (Hunter et al., 2015; IPCC, 2014). A hazard is "the extent and magnitude to which a species or population's environment will be subjected to projected changes" and "Sensitivity is the degree to which a species or population may be impacted, directly or indirectly, by projected changes in climate drivers" (Hunter et al., 2015).

Climate change vulnerability assessments are typically based on scoring systems determined via expert elicitation. Therefore, it is critical that this expert driven process engage a broad group of salmon experts across government, Indigenous communities, academia, etc. In this context PCIC's aim is to provide key knowledge and data inputs to facilitate the vulnerability assessment process. Specifically, PCIC's contribution is to solely focus on quantification of historical and future flow and temperature hazards in freshwater life stages, such as adult migration and egg-to-fry incubation (McDaniels et al., 2010; Healey, 2011). Consequently, this work has focussed on the exploration and development of suitable flow and thermal hazard indicators derived from hydrologic projections that best capture and quantify hazards in the freshwater environment over a large spatial domain and at multiple temporal scales (daily, weekly, monthly, and seasonally). This data would then support assessments of ecological vulnerability to climate change across diverse salmon habitats and populations.

Development of freshwater hazard data adopted two 'scales' of assessment: (a) a fine-scale analysis specifically tagged to representative Sockeye and/or Chinook Salmon indicator stocks (Hyatt et al., 2015; Stiff et al., 2013, 2015a, 2015b, 2017, 2018b, 2018a), and (b) a broader-scale regional analysis at coarser resolution along the entire BC Coast (Figure 1). The broad-scale data, and associated tool, will support regional hazard assessments, whereas the fine-scale streamflow and temperature hazard data will provide a valuable resource for any future vulnerability assessments for the specific indicator stocks.

The following products have been produced:

- Hydrologic projections (streamflow and water temperature) at two scales: (a) gridded broad-scale projections delivered over a large (399400 km^2) contiguous domain, and (b) site-specific fine scale projections for eight study basins. All hydrologic projections are based on an ensemble of climate experiments (multiple GCMs and multiple emissions scenarios).
- A set of broad-scale and fine-scale indicators describing changes in streamflow and water temperature hazards in the freshwater environment due to climate change.

- A software tool, the Salmon Climate Impacts Portal (SCIP), for conducting regional population- and watershed-based hazard summaries based on the broad-scale hazard indicators to support climate change ecological vulnerability assessments.

1.3 Method

The project was divided into three main activities, which are shown schematically in Figure 1 and summarised as follows:

1) Hydrologic modelling to determine climate-driven changes in river discharge and water temperature at two spatial scales:
   a) Broad-scale modelling of British Columbia drainages supporting salmon populations using the VIC-GL model,
   b) Fine-scale modelling of a subset of watersheds using the Raven model.
2) Develop and generate indicators to characterize spatio-temporal freshwater flow and temperature hazards under climate change scenarios, and
3) Develop and deploy the Salmon Climate Impacts Portal to summarise and deliver regional hazard information.

1.4 Report Organization

The report is organized into several sections organized along the main activities. Section 2 describes both the broad-scale and fine-scale study areas. Section 3 describes the hydrologic modelling, including the experimental design (Section 3.1), broad-scale modelling (Section 3.2), and fine-scale modelling (Section 3.3). Streamflow and water temperature hazards are addressed in Section 4, including a description of the hazard indicators utilised (Section 4.1) and results for both the broad-scale and fine-scale study areas (Sections 4.2). The Salmon Climate Impacts Portal, the online tool developed to explore and conduct regional summaries of the broad-scale hazard indicators, is presented in Section 5. Data availability is described in Section 6 and the report concludes with Section 7.

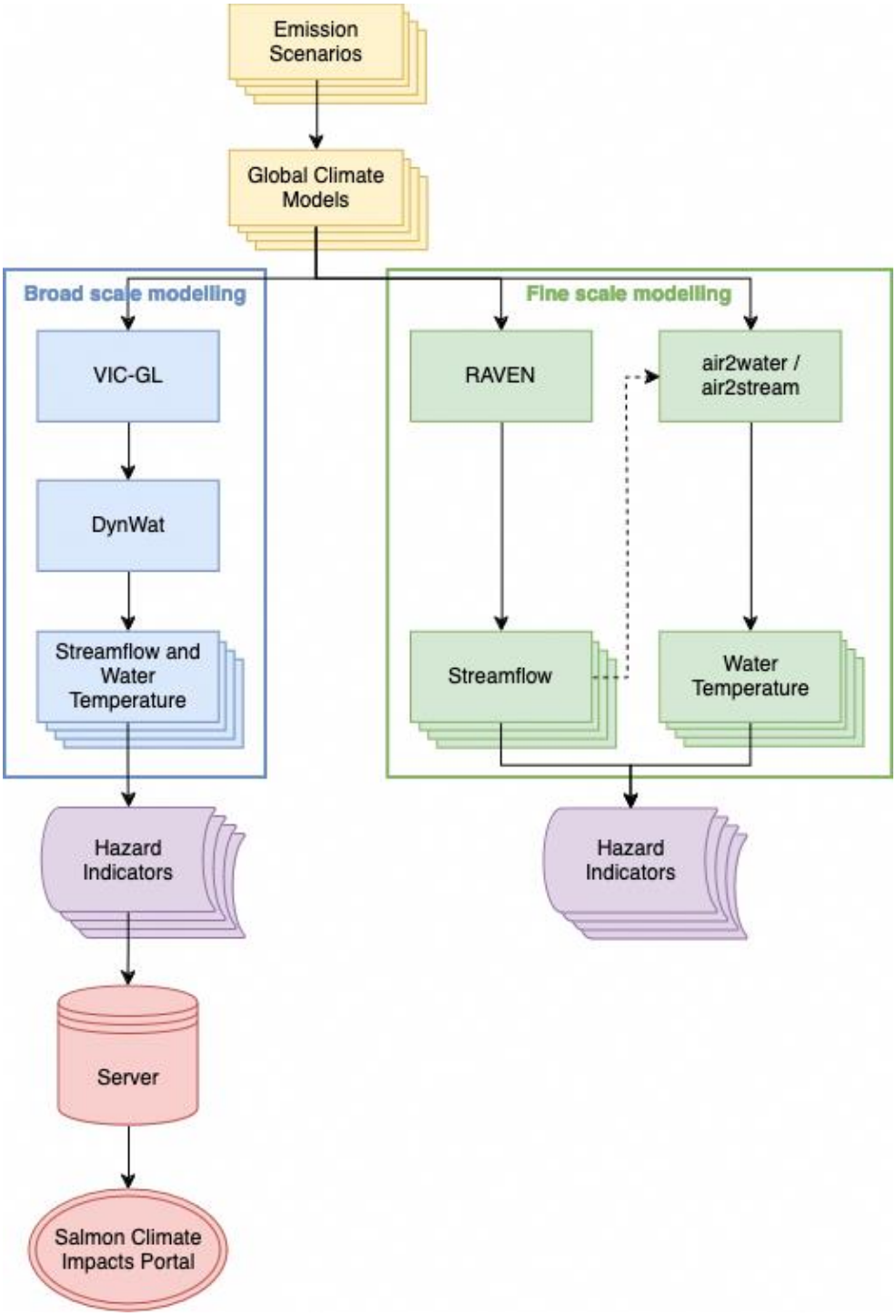

Figure 1. Project methodology showing experimental design (yellow boxes), broad-scale (blue boxes) and fine-scale (green boxes) hydrologic modelling, generation of hazard indicators (purple boxes), and development of the online tool for analysing the broad-scale hazard indicators.

2 Study Domain

2.1 Broad Scale

The study domain, which we term the Pacific Region, includes BC mainland and Vancouver Island areas draining to tidewater along the Pacific Coast (Figure 2). This region incorporates the 'gauged' portion of the study domain, which is the drainage areas upstream of Water Survey of Canada (WSC) hydrometric sites selected for possessing long, reliable data records. This region is home to a wide diversity of salmon species and includes four major basins that drain to sea along the BC coast: Fraser River, Nass River, Skeena River, and Stikine River. Although recent observations have documented potential increases in presence and abundance of Pacific salmon across Canada's Western Arctic (Babaluk et al., 2000; Carothers et al., 2019; Chila et al., 2021), arctic drainages were excluded from the study domain. The study area spans a large geographic region and encompasses a number of distinct ecoregions, defined by physical and ecological features including climate, physiography, oceanography, hydrology, vegetation, wildlife, as well as soil type, flora and fauna communities, and aquatic systems (Demarchi, 2011). Climate change will have impacts across each major drainage basin and the different ecoregions, exposing migrating species, such as salmon, to varying environmental conditions (Caretta et al., 2022; Parmesan et al., 2022). Most of BC's major drainages start along the Pacific coast and extend well into the interior of BC.

Table 1. Watersheds located in broad-scale study area, listed north-to-south.

Mainland Rivers		Vancouver Island Rivers	
Name	Drainage Area (km^2)	Name	Drainage Area (km^2)
Taku	15500	upper Nimpkish	783
Stikine	50900	Tsitika	365
Unuk	1480	Salmon	1210
Nass	18400	Campbell	1470
Skeena (at Usk)	42300	Gold	992
Zymagotitz	376	Oyster	302
Exchamsiks	370	Puntledge	583
Kitimat	1990	Somass	1280
Kemano	556	Englishman	320
upper Dean	3720	Nanaimo	676
upper Bella Coola	4040	Chemainus	355
Wannock	3900	Cowichan	826
Klinaklini	5780	San Juan	580
Homathko	5680		
Squamish	2350		
Mamquam	334		
Fraser	232000		

The study area includes the watersheds (or portions thereof) listed in Table 1. The total size of the modelled drainage area is 399420 km^2, of which the five largest basins (Fraser, Stikine, Skeena, Nass, and Taku) account for 90% of this area.

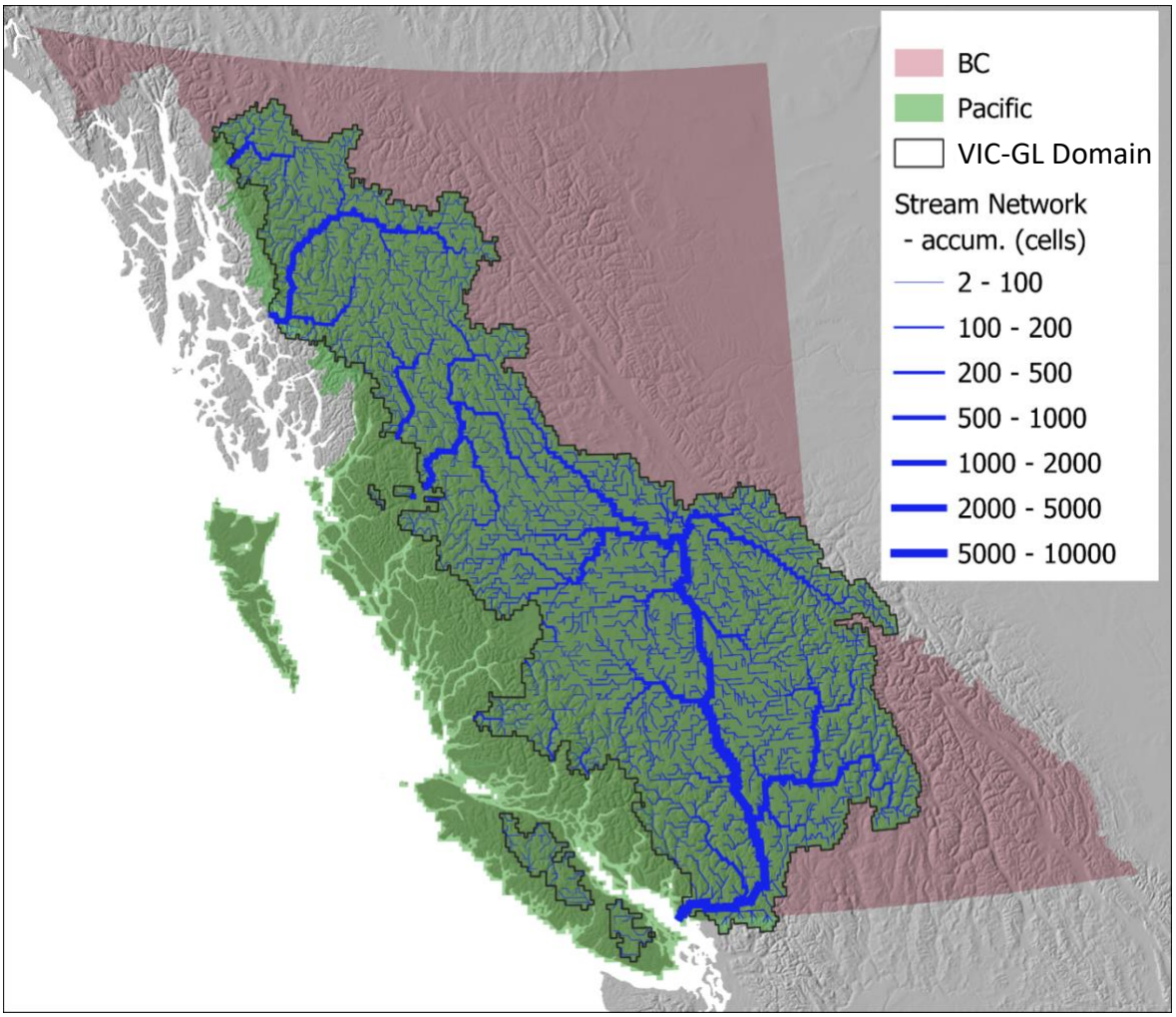

Figure 2. Broad-scale study domain, showing the Pacific Region ('Pacific') and the outline of study domain ('VIC-GL Domain') and provincial outline ('BC'). Also shown is the modelled stream network topology for the VIC-GL domain, where stream network lines are sized by flow accumulation (given as the number of upstream VICGL cells).

2.2 Fine Scale

Eight locations that conform to site-specific detailed salmon population studies were chosen for fine-scale analysis. These sites are shown in Figure 3 and summarised in Table 2, and represent well-studied data rich Conservation Units of Sockeye and Chinook salmon in a subset of watersheds covering most of the BC range of these species.

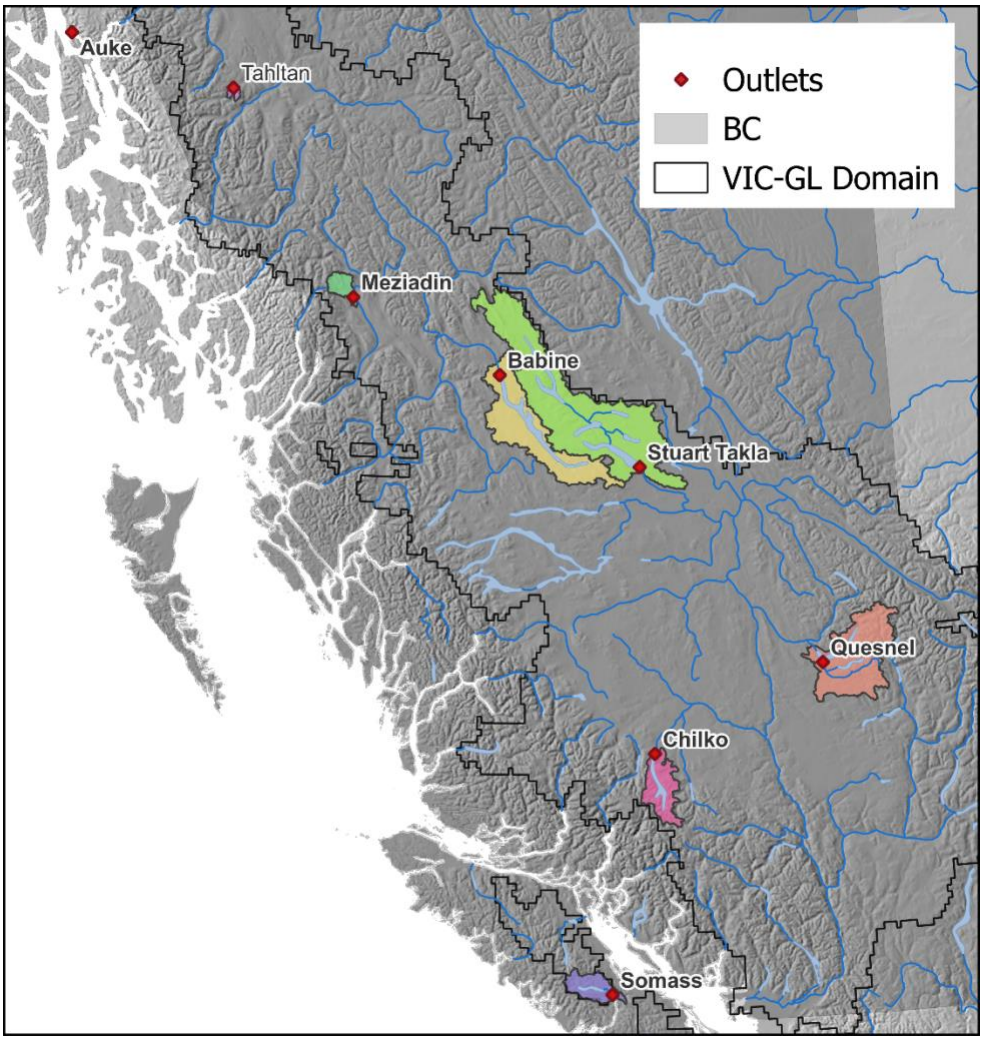

Figure 3. Location of the eight fine-scale study sites.

Table 2. Fine-scale study sites

Name	Outlet Description	Drainage Area (km^2)
Auke	Auke Creek Hatchery weir	10
Tahltan	Outlet of Tahltan Lake	136
Meziadin	Meziadin fishway (located <5km downstream of the lake outlet)	706
Babine	Babine Fence at the outlet of Niltkitkwa Lake	6501
Stuart-Takla	Stuart River at Fort St. James	14407
Quesnel	Quesnel River at Likely	6056
Chilko	Chilko River at stock assessment site near outlet of Chilko Lake	2165
Somass	Somass River at Port Alberni	1419

The Auke Lake watershed is in southeast Alaska approximately 30 km north of the town of Juneau (Figure 3). The study area, which is upstream of the lake outlet, drains an area of 10 km^2. The study area is dominated by the Auke Lake, which has a surface area of 7 km^2 and is just 17 m above sea level. The 323-m Auke Creek flows from Auke Lake to Auke Bay. The watershed supports Sockeye, Coho, Pink, and Chum salmon, as well as Steelhead Trout and Dolly Varden (Stiff et al., 2019).

The Tahltan River is part of the Stikine watershed (Figure 3). The study area is at the outlet of Tahltan Lake, the largest lake in the drainage (approximately 7 km long and 0.5 to 1.25 km wide) and has a total drainage area of 136 km^2. Tahltan Lake has an endemic population of Sockeye salmon and has been stocked since 1990. The watershed is an important producer of Stikine Sockeye salmon (Stiff et al., 2013).

The Meziadin River is located in the Nass River drainage (Figure 3) and is the primary source of Sockeye production (70-80%) in the Nass system (Stiff et al., 2015b). The study area is delineated by the Meziadin fishway (constructed to allow migrating salmon to bypass Victoria Falls to access upstream spawning grounds), located about 5 km downstream of the outlet of Meziadin Lake, which results in drainage area of 706 km^2.

The Babine River is in the headwaters of the Skeena drainage (Figure 3). Babine Lake forms the source of the Babine River and is the largest natural lake in the province with a surface area of 461 km^2. Babine Lake is connected to the downstream Nilkitwa Lake by a 2-km stretch of the Babine River. All species of salmon are present in the Babine River, with Sockeye being the most numerous. The study area is delineated by the Babine River salmon counting fence, which is located one kilometre downstream of the outlet of Nilkitwa Lake at the lower boundary of the Sockeye spawning grounds (Stiff et al., 2015a).

The Stuart watershed is located in the northwestern portion of the Fraser River drainage and consists of three large interconnected lakes, Takla (surface area of 246 km^2), Trembleur (surface area of 117 km^2), and Stuart (surface area of 358 km^2), and associated tributary streams (Figure 3). Two major Sockeye populations, Early Stuart, and Late Stuart, utilize the spawning and lake rearing habitats for incubation and early growth. Early Stuart sockeye spawn in the upper portion of the Stuart Lake watershed in smaller streams tributary to Takla and Trembleur Lakes, and Middle River. Late Stuart sockeye spawn in the rivers between lakes and in tributaries to both these rivers (Levy et al., 2007).

The Quesnel River, with a drainage area of approximately 6600 km^2, is a major tributary of the Fraser River (Figure 3). Chinook, Coho, and Sockeye salmon are all found in the watershed, although Sockeye is the most intensively studied population (Stiff et al., 2018a). The Quesnel watershed contains three main lakes. The fjord-like Quesnel Lake (surface area of 266 km^2) is the largest. The other two lakes are Horsefly Lake (surface area of 59 km^2) and Mitchell Lake (surface area of 21 km^2), which both drain into Quesnel Lake via the Horsefly River and Mitchell River, respectively. The Quesnel watershed supports one genetically-distinct Sockeye population which spawn along the lakeshore of Quesnel Lake and tributaries, within the Horsefly River at its tributaries and in the Mitchell River and its tributaries (Stiff et al., 2018a). The Quesnel study area is delineated by the Water Survey of Canada hydrometric gauge on the Quesnel River at Likely, BC, near the confluence with the Fraser River.

The Chilko River is part of the Chilcotin drainage, which itself is a tributary of the Fraser (Figure 3). The Chilko River begins at Chilko Lake, a 184 km^2 waterbody that is the largest lake in BC above 1000 m elevation. The Chilko River drains north from the lake and the 2165-km^2 study area is delineated by the Department of Fisheries and Oceans stock assessment site located near the lake outlet (Stiff et al., 2017).

The study area supports two populations of Sockeye salmon that spawn either in the Chilko River downstream of the lake or along the lakeshore and its tributaries (Stiff et al., 2017).

The Somass River drains an area of 1419 km^2 into the Alberni Inlet on Vancouver Island (Figure 3). The watershed has three main sub-basins: the Sproat, which is dominated by Sproat Lake that drains via the Sproat River; Great Central, which is dominated by Great Central Lake which drains via the Stamp River; and the Ash River, which drains Oshinaw and Elsie Lakes. The Ash River flows into the Stamp River, which then joins the Sproat River to form the Somass River. The Robertson Creek Hatchery, a Chinook and Coho salmon enhancement facility, is located on the upper Stamp River (https://www.pac.dfo-mpo.gc.ca/sep-pmvs/hatcheries-ecloseries/robertson-eng.html). This facility is now one of the largest on the BC Coast (Hyatt et al., 2015). Both Sproat Lake and, following construction of a fish way on the Stamp River at Stamp Falls in 1927, Great Central Lake support Sockeye salmon. Production levels of four species combined (Chinook, Coho, Pink and Steelhead) make the Stamp/Somass system the largest fish producer on Vancouver Island (Hyatt et al., 2015).

3 Hydrologic Modelling

3.1 Experimental Design

3.1.1 CMIP5 Ensemble

In this section we review the experimental design shared by both the broad-scale and fine-scale hydrologic modelling. Future climate projections at the regional scale start with model simulations of the global climate system. Because these are models, there is inherent uncertainty related to (1) the assumptions about how the greenhouse gases (GHG) will evolve, (2) the climate model and how it represents the physical processes and (3) the internal variability, e.g. the natural variability that we experience as weather or El Nino events, which is irreducible (Arora and Cannon, 2018; Cannon et al., 2020). An ensemble approach has been employed whereby the hydrologic models were forced with simulated meteorological data that was obtained by statistically downscaling climate experiments generated using a range of different global climate models (GCMs) forced by multiple emissions scenarios.

Table 3. CMIP5 global climate experiments

Model ID	Institution	# Runs by Scenario	
		RCP4.5	RCP8.5
ACCESS1-1	Commonwealth Scientific and Industrial Research Organization and Bureau of Meteorology, Australia	1	1
CanESM2	Canadian Centre for Climate Modelling and Analysis, Canada	5	5
CCSM4	National Center for Atmospheric Research, United States	2	2
CNRM-CM5	Centre National de Recherches Météorologiques and Centre Européen de Recherche et Formation Avancée en Calcul Scientifique, France	1	1
HadGEM2-ES	Met Office Hadley Centre, United Kingdom	4	4
MPI-ESM-LR	Max Planck Institute for Meteorology, Germany	3	3

We have used an ensemble of downscaled climate experiments that were already available at PCIC (https://www.pacificclimate.org/data/statistically-downscaled-climate-scenarios) that comprise climate data produced as part of the World Climate Research Programme (WCRP) Coupled Model Inter-comparison Project Phase 5 (CMIP5) (Taylor et al., 2012). These experiments use emissions specified by Representative Concentration Pathway (RCP) scenarios RCP 8.5 and RCP 4.5 (van Vuuren et al., 2011). The RCP 8.5 is a "business as usual" scenario with no explicit policy changes to reduce future emissions, leading to emissions in 2100 that are three times those that we see today. The RCP 4.5 scenario represents an intermediate emissions trajectory whereby radiative forcing stabilizes shortly after 2100 and includes somewhat ambitious greenhouse gas reductions over time. This ensemble is based on a subset of six GCMs selected according to a method (Cannon, 2015), which entails selecting the subset of GCMs that best represent the overall spread of the full CMIP5 ensemble.

Many of the GCMs indicated above have multiple runs available that represent different initial states. The ensemble members with different initial states are usually called realizations, *r*. Using all available

runs from each GCM, the resulting ensemble consists of 32 climate projections (16 each for RCP4.5 and RCP8.5, respectively), which are summarized in Table 3. The original six GCMs, which we refer to as the *PCIC6* ensemble, are based on the following realizations: ACCESS1-0-r1, CanESM2-r1, CCSM4-r2, CNRM-CM5-r1, HasGem2-ES-r1, and MPI-ESM-LR-r3. The ensemble composed of all available runs is termed *PCIC6-full* ensemble. This design of the *PCIC6* ensemble mainly addresses the uncertainty in future projections due to a range of greenhouse gas emissions and that due to differences between GCMs. The *PCIC6-full* ensemble, with multiple realizations for several GCMs, also assesses some additional uncertainty due to internal climate variability (the naturally occurring variations in climate on timescales from daily weather to multidecadal processes due to interactions between various components of the Earth system; Schwarzwald and Lenssen 2022).

3.1.2 Downscaling

The climate response to a prescribed RCP scenario that is obtained from a climate model is of too coarse a spatial resolution, with individual grid cells typically encompassing 10,000 km^2, to be used directly in driving a hydrology model. For example, GCM output at this resolution does not reflect the detailed spatial variation in climate due to local orography and variations in land surface properties that are necessary for simulating surface hydrology well. Therefore, to model changing hydrologic conditions at local and regional scales, daily values of minimum temperature, maximum temperature and precipitation have been statistically downscaled to the resolution of VIC-GL. This downscaling used the Bias Correction/Constructed Analogues with de-trended Quantile mapping reordering downscaling technique (BCCAQv2) (Hiebert et al., 2018) with PNWNAmet (Werner et al., 2019) as the reference meteorology. BCCAQv2 is a hybrid method that combines results from bias-corrected constructed analogs (BCCA) (Maurer et al., 2010) and de-trended quantile mapping (QMAP) (Gudmundsson et al., 2012). BCCA obtains spatial information from a linear combination of historical analogues for daily large-scale fields. QMAP applies quantile mapping to daily climate model outputs interpolated to the high-resolution grid using the climate imprint method of Hunter and Meentemeyer (2005). The BCCAQv2 method includes a revision to the quantile mapping procedure that better preserve changes in quantiles and extremes (Cannon et al., 2015) as compared to its original implementation. BCCAQv2 works well for hydrologic extremes because of its ability to resolve event-scale spatial gradients (Werner and Cannon, 2016). For more information on BCCAQv2 see (Cannon et al., 2015; Hiebert et al., 2018; Sobie and Murdock, 2017; Werner and Cannon, 2016).

3.2 Broad-scale modelling

The broad-scale hydrologic modelling utilised the VIC-GL hydrology model coupled to the DynWat streamflow and water temperature routing model (see broad-scale workflow Figure 1). The resultant output from this workflow was an ensemble of streamflow and water temperature projections on a contiguous computational grid covering the domain shown in Figure 2. Both the VIC-GL and DynWat models are described in detail in a separate deployment report {Citation}, and only a summary is provided in herein. The broad-scale modelling employs the full *PCIC6-full* forcing ensemble.

3.2.1 VIC-GL

Streamflow was simulated with VIC-GL, an upgraded version of the Variable Infiltration Capacity (VIC) model that explicitly models glacier mass balance (accumulation, melt and runoff) and glacier dynamics (change in glacier area) (see Schnorbus 2018 for details). VIC is a spatially distributed macro-scale hydrologic model that calculates water and energy balances in each grid cell. Spatial variability in soil

properties within a drainage basin is modelled by sub-dividing the model domain into a computational grid with a spatial resolution of 0.0625° latitude by 0.0625° longitude (approximately 6 km x 5 km within the study region). The variability of land cover and topography within individual grid cells is further described using hydrologic response units (HRUs) which characterize land surface properties as a function of elevation. VIC runs at a 3-hour temporal resolution and output is aggregated to daily values. Soil moisture processes are represented by three-soil layers, spatial heterogeneity of runoff generation with variable infiltration curves, and subsurface flow generation using the Arno conceptual model (Todini, 1996). Surface runoff is generated when the moisture exceeds the storage capacity of the soil. Water fluxes are computed for a range of hydrologic processes such as evapotranspiration, snow accumulation, snowmelt, infiltration, soil moisture and surface and subsurface runoff. A detailed description of the baseline VIC model is available in Liang et al. (1996, 1994) and Cherkauer et al. (2003).

VIC-GL uses several parametrization strategies to describe the influence of topography and vegetation cover. Sub-grid elevation is described using 200-m elevation bands derived from the GMTED2010 digital elevation model (Danielson and Gesch, 2011). Vegetation classification utilizes the North America Land Cover dataset, edition 2 (Natural Resources Canada / The Canada Centre for Mapping and Earth Observation 2013) produced as part of the North America Land Change Monitoring System (NALCMS). The NALCMS land cover data set divides North America into 19 classes representing circa 2005 conditions, with most forest areas in the region for which VIC-GL has been parameterized being included in a single class, the temperate or sub-polar needle-leaf forest class. This homogeneous region has therefore been further subdivided based on vegetation height and leaf area index. Leaf are index data is from the GEOV1 global time series dataset (Baret et al., 2013; Camacho et al., 2013). Vegetation height is based on global mapping using space borne light detection and ranging (LIDAR) (Simard et al., 2011). The final land cover classification, with needle-leaf forest further sub-divided, contains 22 land cover classes. Although an Ice class exists in the NALCMS-based land cover inventory, the extent and location of glaciers and ice fields was updated using the Randolph Glacier Inventory (RGI) version 3.2 (Pfeffer et al., 2014). Soil classification and parameterization relies on physical soil data from the Soils Program in the Global Soil Data Products CD-ROM (Global Soil Data Task, 2014).

3.2.2 DynWat

The dynamical 1-D water energy routing (DynWat)solves the transport of water and energy in a gridded river network (van Beek et al., 2012; Wanders et al., 2019). For simulating streamflow it is assumed that each grid cell has a single channel reach and discharge in each reach is calculated by the kinematic wave approximation of the Saint-Venant equation (Fread, 1992). This entails that at the end of each time step, a new stage for the simulated discharge is calculated under an assumption of a rectangular channel and passed on to the next time step to estimate the wetted perimeter of the flow and the corresponding roughness coefficient (Dingman, 2015). Waterbodies are treated as contiguous water surfaces with a variable water height and surface area that changes instantaneously with the net inflow over that area, where net inflow is the balance of inflow and outflow. The inflow includes the incoming river discharge and outflow is calculated in analogy to the weir formula as the discharge over a rectangular cross section (Bos, 1989). The discharge at the outlet of waterbodies is added within the time step as lateral inflow to the kinematic wave approximation of the downstream river reach (Wanders et al., 2019).

For calculating the energy balance DynWat assumes that each channel reach experiences full vertical mixing. Within each fully mixed water volume the energy balance is solved by considering the local energy balance plus energy advected by water flowing in and out of the channel reach. For waterbodies, the assumption of complete vertical mixing is invalid. In this case DynWat assumes a model composed of

two well-mixed layers, an upper epilimnion layer and a lower hypolimnion layer. The volume of both layers varies as a function of net inflow. The volume of upper epilimnion layer is set by assuming a constant layer thickness (or thermocline depth), which is determined as a function of waterbody fetch length, and the hypolimnion constitutes the remaining waterbody volume. Surface energy exchange and lateral advection of energy occurs exclusively in the epilimnion layer. Energy is distributed between the two layers by assuming the hypolimnion temperature remains fixed at 4°C, which corresponds to the temperature of maximum water density. The temperature of the epilimnion layer is determined by solving the resultant energy balance. The DynWat model also includes processes for the formation and breakup of ice cover and dynamic coupling of surface water abstraction and reservoirs operations. The model can simulate daily water temperatures with 5 min (or finer) temporal disaggregation to ensure stable model simulations in smaller streams and lakes (Wanders et al., 2019). At PCIC additional modifications have also been made to simulation of the energy balance, river ice, and estimation of waterbody outflow (Schnorbus, 202).

In our implementation the DynWat model is used in a stand-alone configuration to allow off-line coupling with the VIC-GL model. In this case DynWat is supplied with the following hydrological inputs:

1. surface runoff from rainfall,
2. surface runoff from snow or glacier melt, and
3. baseflow or groundwater discharge.

The temperature of surface runoff and baseflow also must be specified. The baseflow temperature is assumed equal to the soil temperature, where soil temperature is estimated as a function of air temperature using the method of Mohseni et al. (1998). Surface runoff from rainfall is set to the air temperature and surface runoff from snow- and ice-melt is set to a fraction, *f*, of the soil temperature. The model also needs additional information on the meteorological input, such as temperature, precipitation, and radiation terms. The DynWat model runs on the same computational grid as VIC-GL, with the resultant stream topology shown in Figure 2. In the current implementation of DynWat all reservoirs treated as natural lakes. Hence, in those stream reaches affected by flow regulation the resultant streamflow and water temperature values reflect hypothetical natural conditions.

A full description of the model is available in Wanders et al. (2019) and recent modifications undertaken at PCIC are described in the (Schnorbus, 2024).

Several physical properties of the routing system are prescribed via parametrization. The slope for each stream reach was estimated from GMTED2010 digital elevation model (Danielson and Gesch, 2011). Waterbody surface area was obtained from the BC Freshwater Atlas (Ministry of Forests, 2024). Values of waterbody capacity, and maximum depth were obtained from lake and reservoir bathymetry data collected from various sources, although data for most lakes was obtained from bathymetric maps published by the government of British Columbia (Government of British Columbia, 2024). The channel network topology is determined by assigning a ‘dominant’ flow direction to each grid cell where runoff from each cell can only flow in one of eight flow directions (N, NE, E, SE, S, SW, W or NW) to a neighbouring cell. Flow directions were obtained from the Dominant River Tracing (DRT) product (Wu et al., 2012). Additional physical properties are assigned via model calibration. These include manning’s roughness, kinematic wave parameters, parameters that describe the allometric relationship between channel width and discharge (e.g. Knighton, 1998), and the parameters that describe the baseflow

temperature as a function of air temperature. Deployment of the DynWat model, including calibration, is detailed in Schnorbus (2024).

3.3 Fine-scale modelling

The fine-scale hydrologic modelling utilised the Raven hydrological modelling framework and the separate air2water and air2stream water temperature models (see fine-scale workflow in Figure 1). The resultant output from this workflow was an ensemble of streamflow and water temperature projections at specific points within the study sites shown in Figure 3. Both the Raven and air2water/air2stream models are described in detail in the Raven deployment report (Schoeneberg et al., 2023), and only a summary is provided in the following sections. Fine-scale modelling is limited to the *PCIC6* forcing ensemble.

3.3.1 Raven

Raven is a robust and highly generalized object-oriented hydrological modelling platform(Craig et al., 2020). The structure and organization of the model has been designed to accommodate flexibility in defining model structures, process representations, spatial discretization approaches, interpolation methods, and numerical algorithms. The software includes over 100 hydrological process algorithms and Raven's plug-and-play architecture allows straightforward addition of new hydrologic process or forcing function estimation algorithms. The Raven framework and the philosophy behind it are presented in detail by Craig et al. (2020).

Raven has been demonstrated to successfully emulate several popular hydrological models, and one such model is the UBC Watershed Model (UBCWM). The UBCWM is suitable for modelling streamflow in the many snowmelt-dominated watersheds of BC (Morrison et al., 2002; Quick and Pipes, 1977). We deployed Raven-UBCWM, with Raven v3.5, which allows lakes to be parameterized or Raven v3.7, which allows Raven to be coupled to the Regional Glaciation Model (RGM), if glaciers are present. This modelling framework builds on recent studies of climate change impacts in BC, including the fully-distributed version of Raven-UBCWM needed to couple to a dynamic glacier model (Tsuruta and Schnorbus, 2022, 2021). Deployment of the Raven model, including calibration, is detailed in Schoeneberg et al. (2023).

3.3.2 Air2stream / air2water

Water temperature was modelled at the eight watersheds of interest at the locations listed in Table 4. All sites except Stamp Fall Fishway are located at the outlet of lakes. Therefore, air2water, a lake surface temperature model, is used (Piotrowski et al., 2022) for all sites except Stamp Falls. Air2water simulates water temperature based on air temperature. The air2stream model, a version of the model adapted for stream water temperature modelling (Toffolon and Piccolroaz, 2015), is used at the Stamp Falls Fish way (Table 4). This model estimates water temperature based on air temperature and discharge.

In this study, we use air2water v2.0 downloaded from https://github.com/spiccolroaz/air2water. This model relies on air temperature only to estimate lake surface water temperature. The air2water model is derived from the volume-integrated heat balance equation applied to upper volume of the lake that is affected by heat exchange with the atmosphere. The model is described by the following ordinary differential equation:

$$\frac{dT_w}{dt} = \frac{1}{\delta}\{a_1 + a_2 T_a - a_3 T_w + a_5 \cos\left[2\pi\left(\frac{t}{t_y} - a_6\right)\right]\} \quad (1)$$

$$\text{with: } \begin{cases} \delta = \exp\left(-\frac{T_w - T_h}{a_4}\right) & for\ T_w \geq T_h \\ \delta = \exp\left(-\frac{T_h - T_w}{a_7}\right) + \exp\left(-\frac{T_w}{a_8}\right) & for\ T_w < T_h \end{cases} \quad (2)$$

where t is time, T_w and T_a are water temperature and air temperature in °C, δ is a dimensionless parameter which represents the ratio between the average depth of the surface layer and that of a reference layer, t_y is the duration of a year in the units of time considered in the analysis (here days), T_h is the reference value of the deep-water temperature, and a_1-a_8 are the model parameters. Equation (1) represents the combined effect of meteorological variables, particularly the coefficient $\hat{a}_5$ which integrates the seasonal variability of external forcing variables other than air temperature. It is associated with the amplitude of the annual variations of the solar radiation. Equation (2) emulates the progressive thinning of the surface water volume affected by the heat budget when the lake is stratified (first formula) and when the lake is inversely stratified (second formula).

Table 4. Water Temperature Study Sites.

Basin	**Site**
Auke	Auke Creek Hatchery weir
Tahltan	Outlet of Tahltan Lake
Meziadin	Meziadin fishway (located <5km from the lake outlet)
Quesnel	Quesnel at Likely
	Lower Horsefly River above Quesnel Lake
Babine	Babine Fence at the outlet of Niltkitkwa Lake
Somass	Sproat River at the outlet of Sproat Lake
	Stamp River at the outlet of Great Central Lake
	Stamp River at the Stamp Falls fishway
Stuart-Takla	Stuart River at Fort St. James
Chilko	Chilko River at DFO stock assessment site

4 Freshwater Hazards

4.1 Hazard Indicators

Climate change across freshwater systems will impact watershed hydrology through changes in baseflow, evapotranspiration, precipitation, rainfall, and snow melt, to name a few mechanisms. While these may change the dynamics of freshwater systems, previous studies have identified that salmon will be most affected directly by changes in temperature and discharge (Hyatt et al., 2015; Stiff et al., 2018b).

It is well known that temperature is one of the biggest climate change-related threats to ecosystems and society (IPCC, 2021), and salmon are no exception. Many studies have shown that warming temperatures pose one of the greatest risks to the survival of salmon populations (Crozier et al., 2019, 2020; Hinch and Martins, 2011; Hyatt et al., 2015). High temperatures can negatively affect egg mortality, alevin development, and egg maturation; high temperatures during the smolt phase can cause premature smolting, desmoltification, and shifts in emigration timing; elevated temperatures can create thermal blockages that result in adult and juvenile migration delays; and in the extreme, very high temperatures can be outright lethal to salmon (see Richter and Kolmes, 2005 and references therein). With increasing water temperature water quality generally decreases and many fish diseases are also exacerbated (Richter and Kolmes, 2005).

Impacts on salmon due to changes in flow tend to differ across life stages. Changes in flow have been observed to affect swim speed and migration timing and success of adults, especially at extreme low or high flow (Hinch and Martins, 2011; Quinn et al., 1997; Salinger and Anderson, 2006; Sykes et al., 2009). High flows can have a positive or negative effect, depending upon life stage (Crozier et al., 2019). High flows can benefit migrating smolts, but can displace sediment and scour eggs from redds (Crozier et al., 2019; Hinch and Martins, 2011; McDaniels et al., 2010; Wainwright and Weitkamp, 2013), affecting rates of egg-to-smolt survival (Shanley and Albert, 2014). Summer low flow and drought can reduce habitat availability and sever connections between habitats, causing mortality from stranding (Crozier et al., 2019). Low flows can also contribute to elevated water temperature and reduced water quality. Salmon life history strategies represent an adaptation to the freshwater environment, and one of the most fundamental characteristics of this environment is the seasonality of streamflow (Beechie et al., 2006; Waples et al., 2001). Therefore, changes in the hydrologic regime (rainfall- versus snowmelt-dominated) will alter the seasonality of streamflow, raising the possibility of maladaptation under such circumstances.

A suite of 10 freshwater hazard indicators have been selected for analysis and for inclusion in the online tool (see Section 5). These indicators were chosen based on both literature review and discussion with colleagues from the Department of Fisheries and Oceans (H. Stiff and S. Grant, personal communication, 2021). These indicators address both flow and thermal hazards and cover a range of temporal scales from daily, monthly, and annual. The indicators are meant to be somewhat generic and, therefore, applicable across a broad region and a wide range of salmon populations. Therefore, we have avoided indicators that tend to be overly species- and/or population specific, and those which are tied to very specific dates, periods, or life stages (e.g. Marsha et al., 2021 and references therein). Although the selected indicators will not fit every need, they should nevertheless provide a solid regional overview of the range of freshwater hazards encountered by salmon both historically and under the impact of future climate change.

Streamflow and temperature hazards were estimated based on several quantitative indicators to highlight hazards to various aspects of the biology and survival of salmon (Table 5). Moderate changes in temperature may have impacts on growth and fecundity, but minimal effect on survival, thus mean temperature may be best suited to measure risk to these aspects of salmon biology. For this we used two indicators: mean daily (*tw_day*) and mean monthly (*tw_month*) water temperature. However, temperatures above a threshold have been found to have significant effects on survival (Hyatt et al., 2003; Mantua et al., 2010; Stiff et al., 2018b) and peak-over-threshold (POT) indicators are best suited to measure such risks (Hyatt et al., 2015; Stiff et al., 2018b). A temperature of 19 °C was selected as the threshold. This temperature is above the thermal limit at which embryonic development and smoltification become adversely affected (12 - 17 °C); at the low end of the range for thermal blockage for both juvenile and adult migration (18 – 24 °C); but below the lethal limit for juveniles and adults (approximately >23 °C) (all species) (Mayer et al., 2024; Richter and Kolmes, 2005). This temperature also tends to lie at the upper range of optimum temperature for aerobic scope across species (14 - 21 °C) (Mayer et al., 2024). Two temperature threshold indicators were developed, the number of days per year above 19 °C (*POT19freq*), and the mean spell length per year above 19 °C (*POT19dur*). Mean daily (*flow_day*) and monthly flow (*flow month*) was used as a general indicator of changes in streamflow (Crozier et al., 2019). High- and low- flow hazards were characterized based on the historical probability distribution, and we used the number of days when streamflow was > 95th-percentile and < 5th-percentile of historical streamflow as indicators of high (*highQ95*) and low (*lowQ05*) flow hazards, respectively. Hazard due to extreme high flow was also characterized by the magnitude of annual maximum peak flow (*peakQmag*). In rain-dominated basins, annual maximum peak flows occur in fall or winter, during the storm season along the west coast; in snow-dominated basins, peak flows occur during the spring freshet. In hybrids basins, high flows occur due to both major rain events in fall and early winter, and to snowmelt during spring. Therefore, the annual maximum peak flow date was used as a convenient indicator of hydrologic regime change (*peakQday*).

Table 5. Description of hazard indicators

Hazard	Indicator	Climatology	Units	Description
Streamflow	*flow_day(p,d)*	Daily	m^3s^{-1}	Daily flow per day of year (*d* = 1, …, 365)
	flow_month(p,m)	Monthly	m^3s^{-1}	Monthly flow (*m* = 1, …, 12)
	peakQmag(p)	Annual	m^3s^{-1}	Magnitude of annual maximum peak flow
	peakQday(p)	Annual	doy	Day of annual maximum peak flow
	highQ95(p)	Annual	days	Annual number of days of flow > 95th percentile of historical flow
	lowQ05(p)	Annual	days	Annual number of days of flow < 5th percentile of historical flow
Temperature	*tw_day(p,d)*	Daily	°C	Daily water temperature per day of year (*d* = 1, …, 365)
	tw_month(p,m)	Monthly	°C	Monthly water temperature (*m* = 1, …, 12)
	POT19freq(p)	Annual	days	Annual number of days with water temperature > 19°C

POT19dur(p)	Annual	days	Annual duration (consecutive days) of water temperature > 19°C

For the broad-scale, indicators were calculated as gridded values at a spatial resolution of 0.0625°. To capture future changes the indicators were calculated as climatological values for four 30-year periods, *p*, 1971-2000 (historical baseline), 2011-2040 (early-century), 2041-2070 (mid-century), and 2071-2100 (end-century). For each period every indicator was calculated as the 30-year mean, minimum, maximum, and standard deviation for each grid cell, for a total of 160 calculated indices for each ensemble member, and a total of 5120 indices over the full *PCIC6-full* ensemble.

For the fine-scale study, and identical set of hazard indicators have been produced for the sites identified in Table 4.

4.2 Results

4.2.1 Broad scale

Although indicators are available for each individual member of full 32-member *PCIC6-full* forcing ensemble, for visualization purposes results in this section show the ensemble means based on the smaller *PCIC6* ensemble. Specifically, for each period and each emissions scenario for any given indicator, the figures display the average across the six (one for each GCM) climatological means.

Specific runoff (runoff/unit area) is higher in wetter climates than it is in drier climates, so for an equal size drainage area, wetter climates produce larger magnitude flood events. Therefore, at the local scale (about 100 km^2), the spatial distribution of peak flow magnitude will be broadly consistent with precipitation climatology (Figure 4). However, as runoff is integrated over increasingly larger scales, peak flow magnitude in larger basins tends also to increase with increasing drainage area. Consistent with the topology depicted in Figure 2, the largest peak flow values occur where flow concentrates along major tributaries and the main stem of the Taku, Stikine, Skeena, and Fraser Rivers. Changes in peak flow magnitude at each grid cell will be influenced by numerous factors, the relative importance of which vary as a function of spatial scale. For cells draining very small drainage areas, individual grid cell changes will be affected more by local elevation, relief, and changes to the local climate, whereas peak flow changes in cells draining larger areas are likely influenced by changes occurring in distant (potentially wetter) upstream locations. Consequently, at the individual cell scale the spatial patterns of peak flow change at mid- and end-century displays a rather heterogeneous pattern, although the northern portion of the domain tends to display a more coherent pattern of increasing peak flow (Figure 4). Spatial heterogeneity is also affected by noise resulting from model error and calibration artifacts, as well as natural variability.

Much of the study domain experiences a nival peak flow regime (annual maximum peak flow is predominantly due to spring-summer snow melt) during baseline period (1971-2000) such that the interior the Fraser drainage tends to experience peak flow occurrence in late spring (May-June), whereas occurrence in the Coast and Rocky Mountains is later in June-July (Figure 5). On the more glaciated windward side of the Coast Mountains, peak flow tends to happen later in the summer during July – August (Figure 5). Rainfall-dominated areas along the outer coast, Vancouver Island, and parts of the Lower Mainland, the annual peak flow typical occurs during winter storm events (November – January; Figure 5). At mid- and end-century historically snowmelt-dominated regions (most of the Fraser and BC

Coast interior) will experience a shift to earlier snowmelt and earlier peak flew occurrence (Figure 5). Nevertheless, mean occurrence of peak flow in early spring in these regions suggests that the peak flow regime will still be snowmelt-dominated. Very little change in peak flow timing is expected to occur in historically rainfall-dominated regions along the outer coast.

The mean annual number of days where flow exceeds the historical (1971-2000) 95th flow percentile is shown in Figure 6. For the baseline period the frequency, by definition, is 18.25 days (0.05 x 365 days). At mid-century the domain shows a mixed response where many parts of the domain will experience more frequent high flow days, much of the area will see little to no change, but some parts of the Fraser will experience less frequent high flow days. The direction of change is similar by end-century, although the magnitude of change is larger. There does appear to be a weak north-south gradient, where the northern portion of the domain is expected to get wetter, and the south is expected to get drier. There are also some areas of spatial coherence to the projected change, where high flow days are expected to become more frequent in the lower Stikine-Iskut, but less frequent along the southern Coast Mountains and Rocky Mountains (Fraser; Figure 6).

The PCIC6 ensemble for the mean annual number of days where flow is below the historical (1971-2000) 5th flow percentile is shown in Figure 7. As per high flow days the baseline value is, by definition, 18.25. At mid- and end-century it is projected that most of the domain will experience a lower frequency of low flow days, and the frequency may drop to zero over much of the area. However, there are some regions where opposite is expected, such as Vancouver Island, the Lower Mainland, and a large portion of the upper Fraser and Nechako watersheds.

Results for the number of hot days (i.e. days in which daily stream temperature exceeds 19°C) indicates that water temperature is expected to increase from baseline through mid- and end-century (Figure 8). During the baseline period some parts of the Fraser already experience anywhere between 1 to over 40 hot days, particularly in the South Thompson and regions bordering the middle Fraser. At end-century the area experiencing hot days is projected to increase, but not substantially compared to mid-century, although almost the entire domain will experience some hot days for RCP8.5. Some spatial patterns are evident in the results: the southern portion of domain is warmer than the north, regardless of period or scenario, and higher elevation regions will remain cooler than low-elevation regions. The climate response is also stronger for RCP8.5 than RCP4.5. Many of the tributary rivers in the Fraser drainage are expected to experience the greatest frequency of hot days (Figure 8).

The mean annual spell length for hot days (i.e. mean duration of days with water temperature more than 19 °C) is shown in Figure 9. The results for the mean spell length accord very closely with the frequency of hot days, i.e. the mean duration of hot days is expected to increase with future warming, and changes will be larger at end-century than mid-century, and larger for RCP8.5 than RCP4.5. The longest spell lengths are again expected to occur in the Fraser, most likely due to the prevalence of large lakes and reservoirs that maintain a strong thermal inertia (e.g. Nechako, Quesnel, and Stuart-Takla).

A clear signal of increasing water temperature with increasing climate warming is also evident on a monthly scale (Figure 10). Results for monthly mean water temperature for end-century, using sample months of January (winter), April (spring), July (summer), and October (fall), show that warming is to be expected throughout the year. However, in winter, the area affected will be confined to Vancouver Island and the Lower Mainland, as water temperature in the rest of the study area will remain close to freezing (see January in Figure 10).

End-century changes in monthly mean streamflow show a very distinct seasonal pattern over the study area (Figure 11). End-century results for January (winter), April (spring), July (summer), and October (fall) show an overall trend of increased monthly streamflow in January and April, decreased flow in July, and increased flow in October. This overall pattern is explained by an expected increase in both temperature and precipitation in the fall and winter that will result in increased rainfall throughout the domain (e.g. January and October in Figure 11), an earlier snowmelt freshet in spring which explains increased flow in April over most of the area, decreased precipitation in summer resulting in lower streamflow. Nevertheless, there are local exceptions to this general trend. For example, flow is projected to decrease over parts of Vancouver Island in April (more so for RCP8.5 than RCP4.5), whereas flow near the outlet of the Stikine-Iskut is projected to increase in July and some parts of the Fraser and mid-coast, particularly for RCP8.5 (Figure 11).

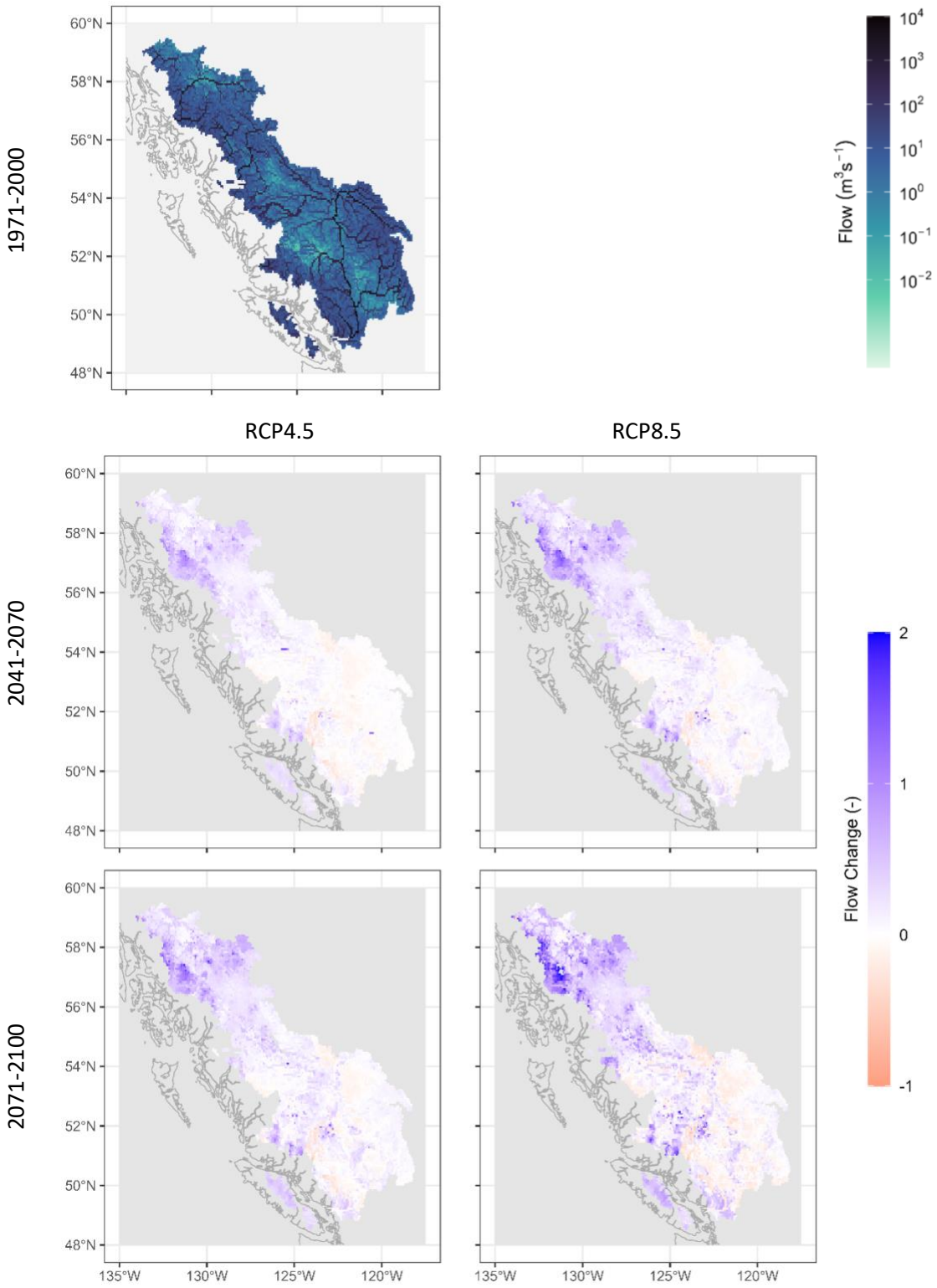

Figure 4. Ensemble mean of mean annual maximum peak flow magnitude (1971-2000) and ensemble mean projected change for mid- and end-century. Note that fill colors for the baseline (1971-2000) period are plotted on a logarithmic scale.

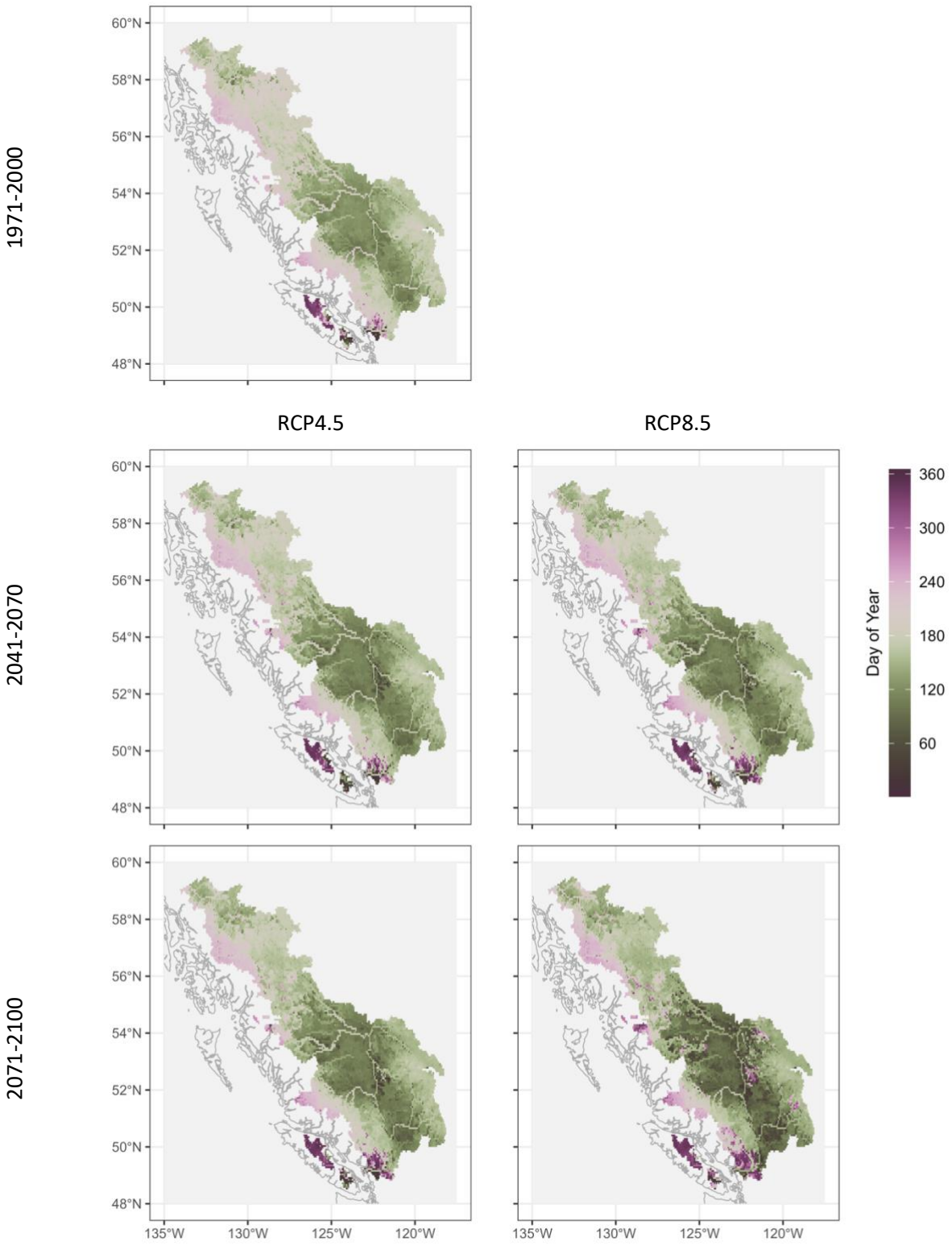

Figure 5. Ensemble mean of mean day of year of annual maximum peak flow occurrence.

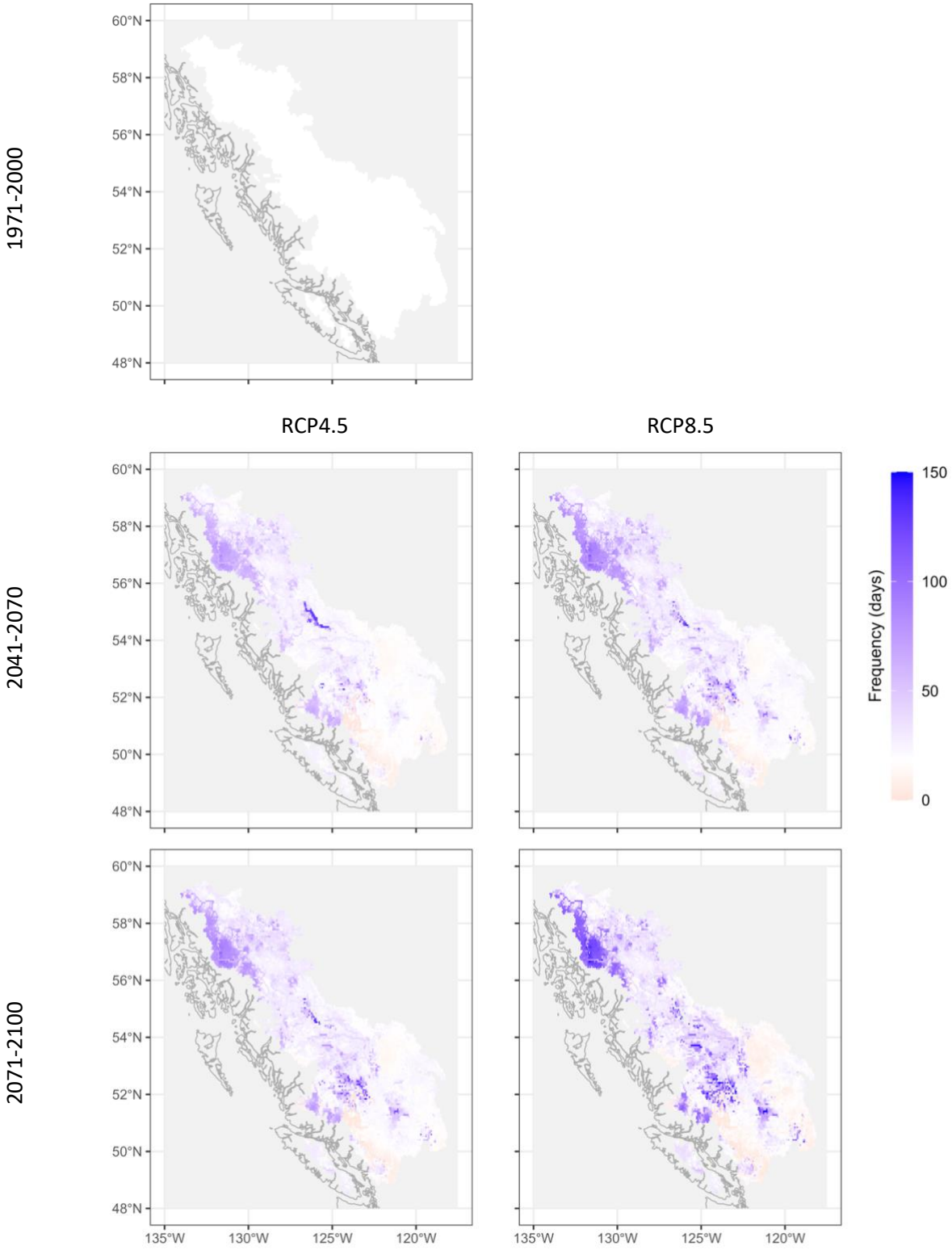

Figure 6. Ensemble mean of annual mean number of days where flow exceeds the historical (1971-2000) 95th flow percentile. Note that, by definition, the baseline historical frequency is 18.25 days. Blue indicates wetter (increasing number of days) and red indicates drier (decreasing number of days).

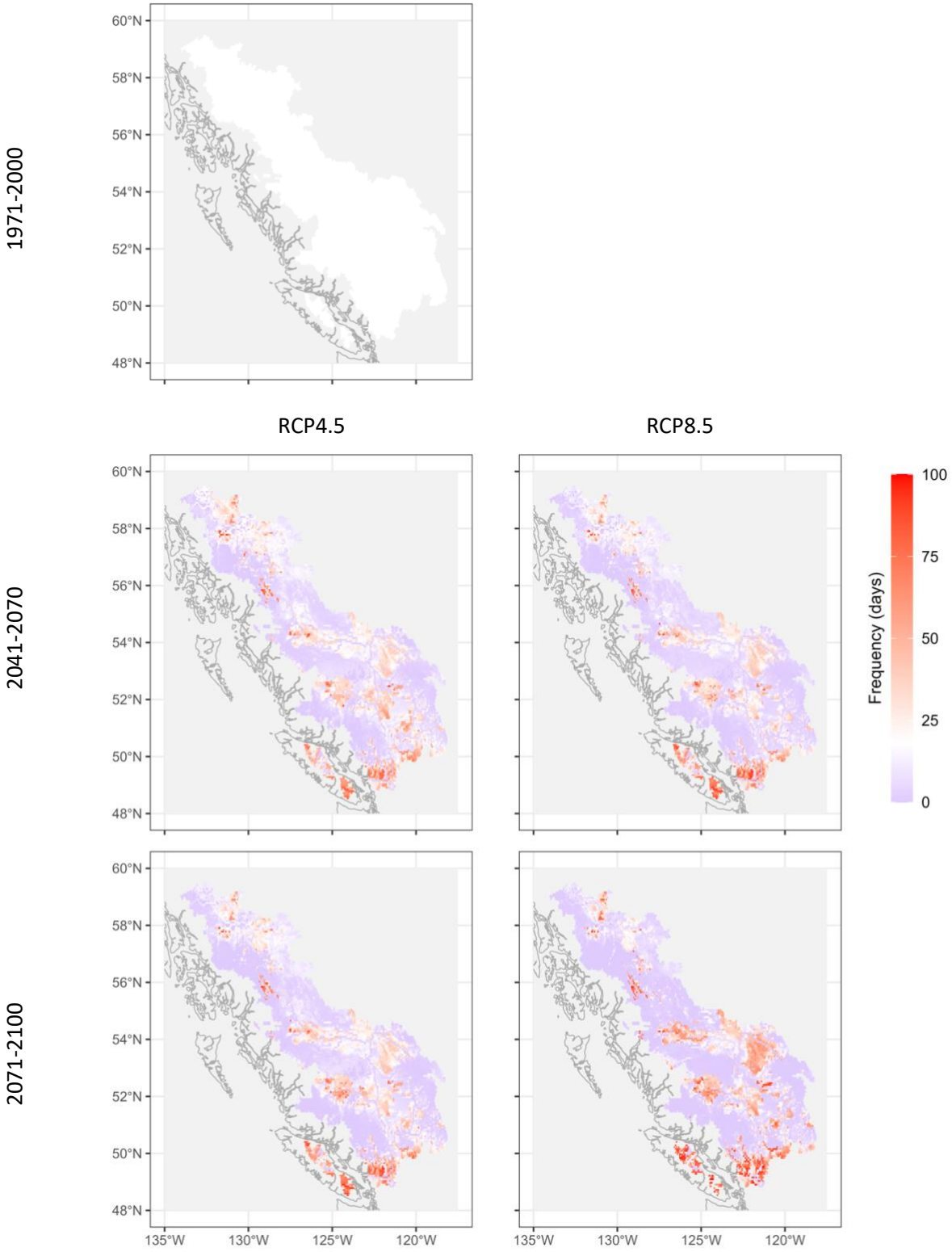

Figure 7. Ensemble mean of annual mean number of days where flow is below the historical (1971-2000) 5th flow percentile. Note that, by definition, the baseline historical frequency is 18.25 days. Blue indicates wetter (decreasing number of days) and red indicates drier (increasing number of days).

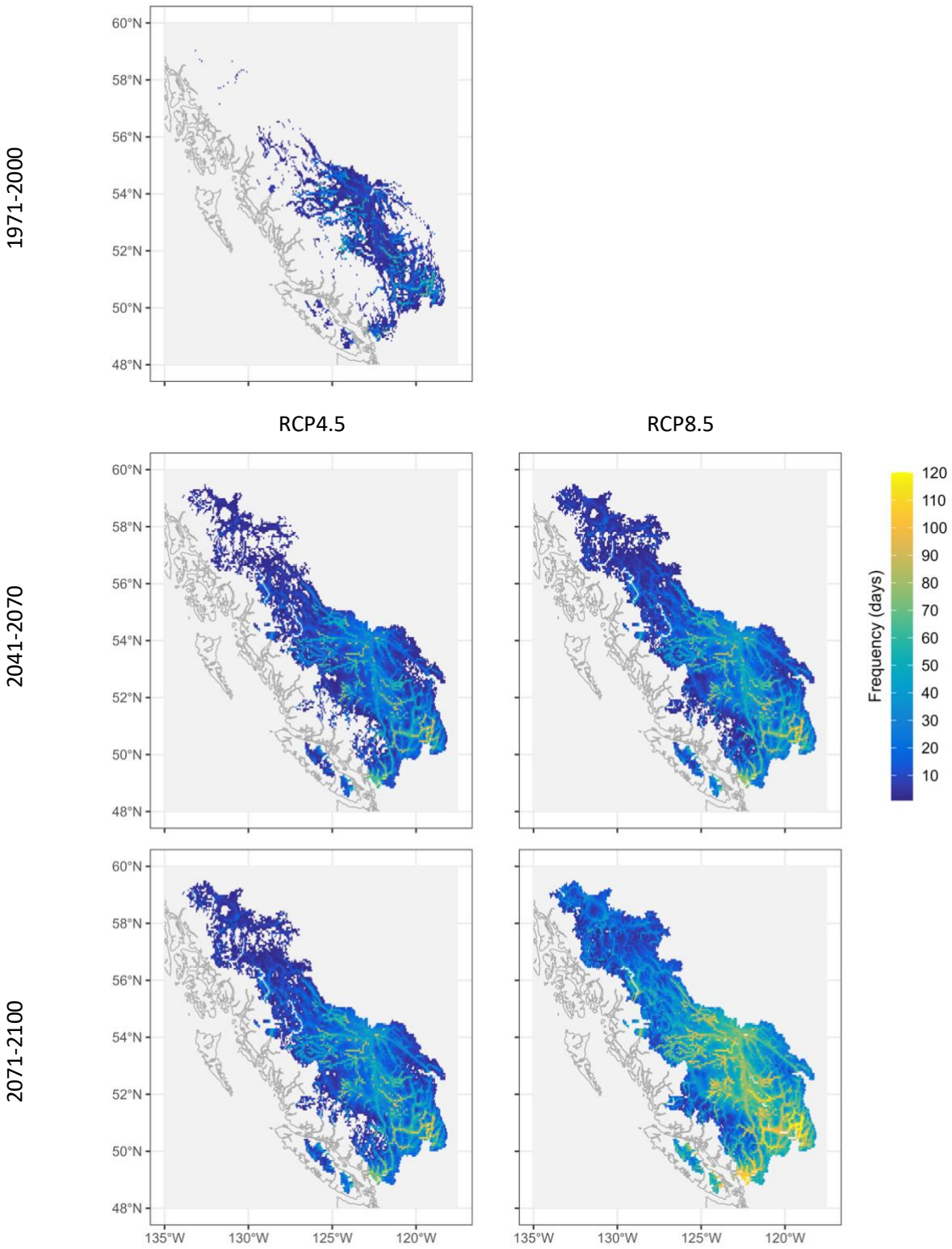

Figure 8. Ensemble mean of annual mean number of days that daily stream temperature exceeds 19 °C. Only values > 0 days are displayed.

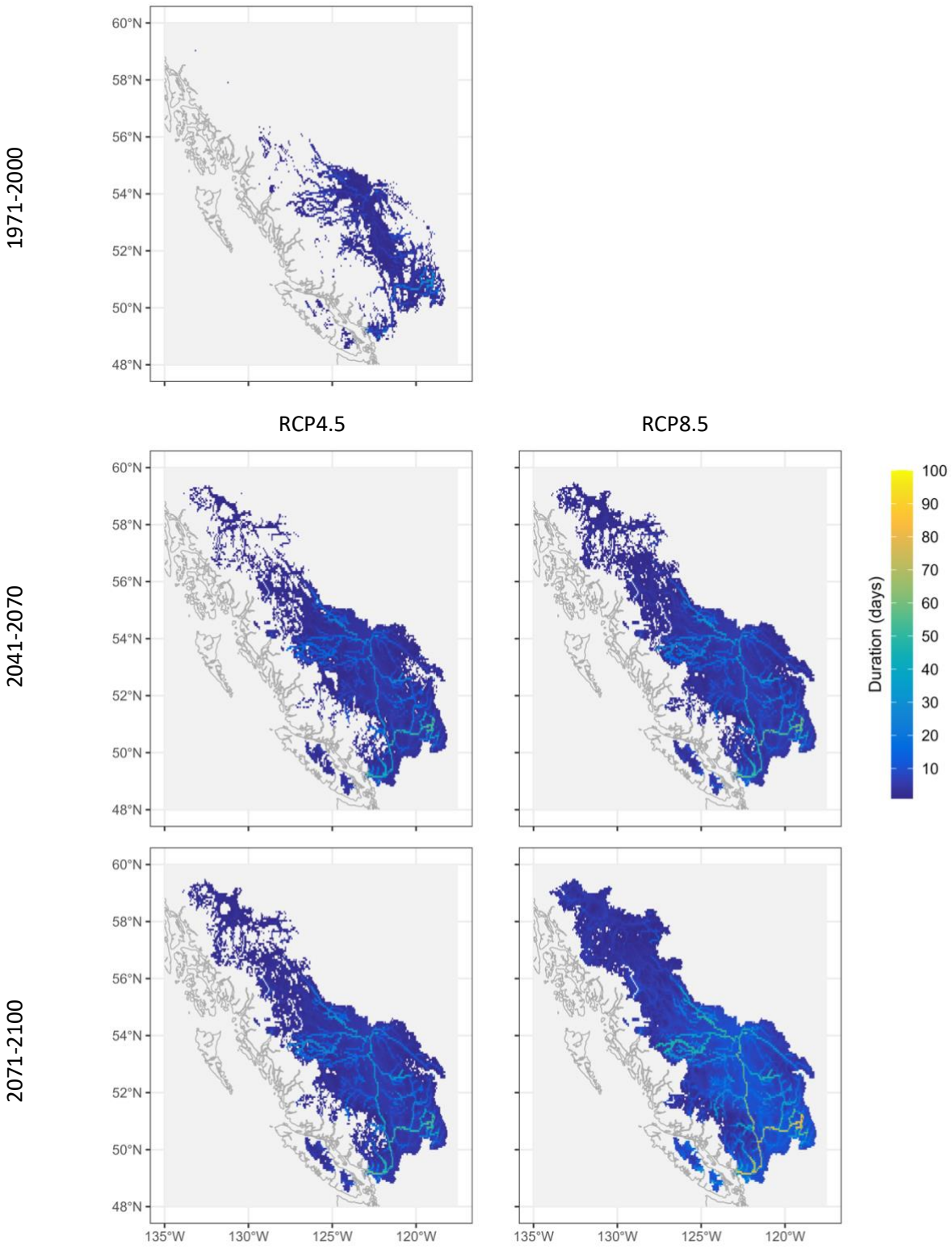

Figure 9. Ensemble mean of annual mean spell length of days that daily stream temperature exceeds 19 °C. Only values > 0 days are displayed.

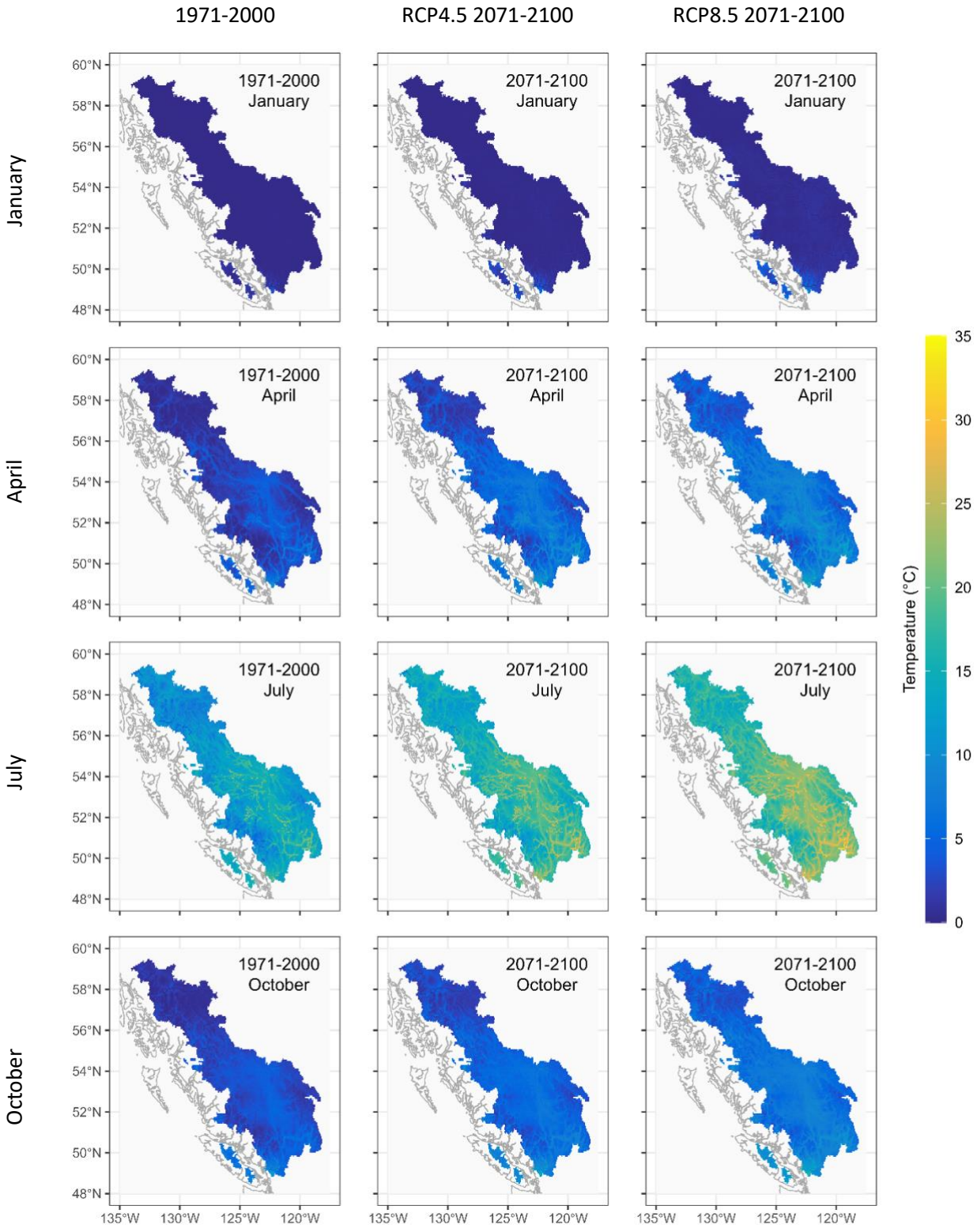

Figure 10: Ensemble mean of monthly mean water temperature.

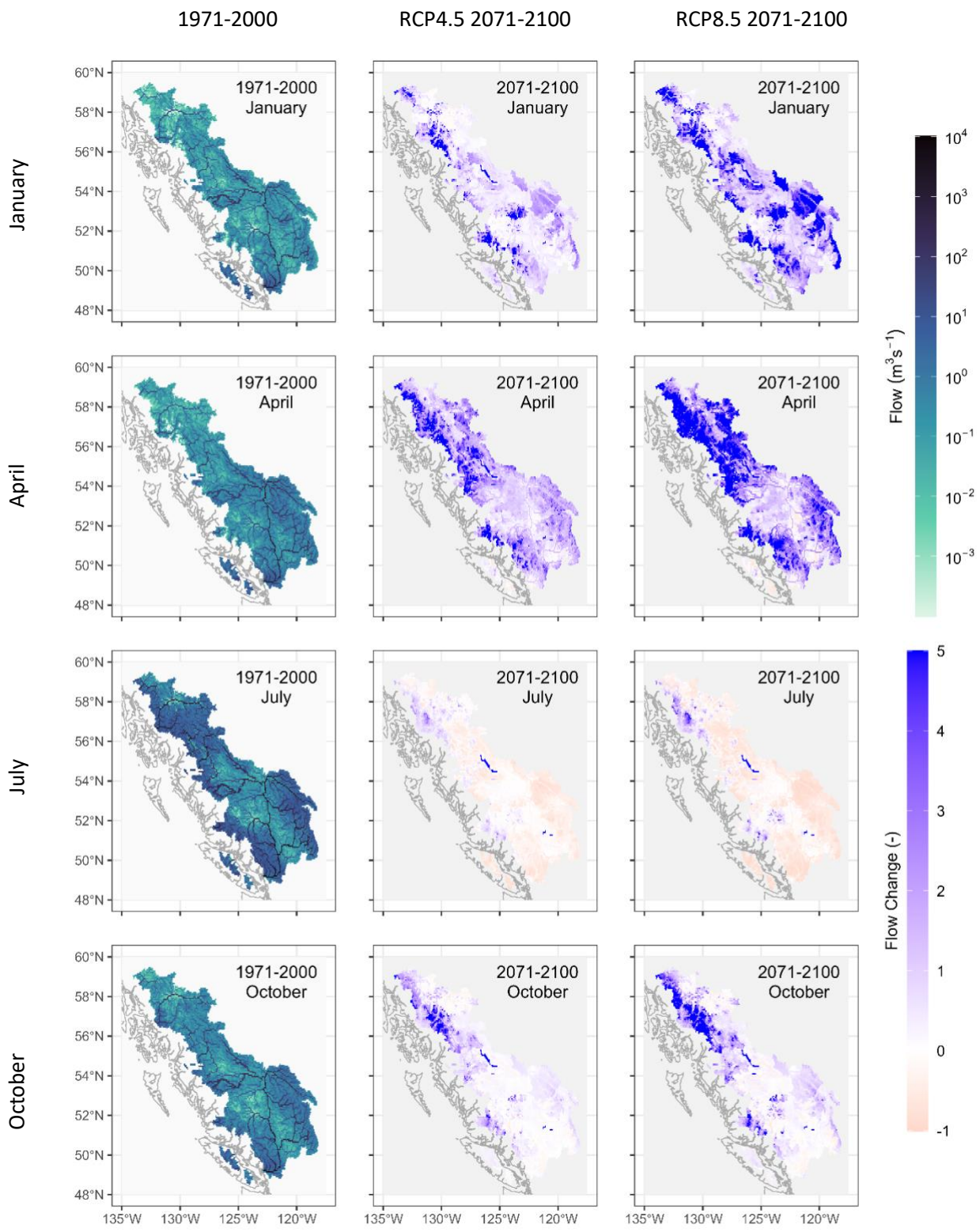

Figure 11: Ensemble mean of monthly mean streamflow (1971-2000) and ensemble mean of projected change in monthly streamflow at end-century (2071-2100). Note that fill colors for the baseline (1971-2000) period are plotted on a logarithmic scale.

4.2.2 Fine scale

Streamflow and water temperature hazard indicator results are shown for the outlet of each study area (Table 2).

The results for mean daily flow for end-century are given in Figure 12. For sites with historically nival or nival-glacial streamflow regimes (i.e. Tahltan, Meziadin, Babine, Stuart, Quesnel, and Chilko) flow is expected to increase in the fall and winter (due to increased rainfall), the snowmelt freshet will begin and peak earlier in the year, and streamflow in the summer is expected to decrease as a results of an earlier depletion of snow storage and, in certain locations, decreased summer precipitation. For the Somass, which has a rainfall-dominated streamflow regimes, streamflow is projected to increase during the fall and winter, due to increasing rainfall, but decrease in summer due to decreasing rainfall. Streamflow in the Auke, which historically has a hybrid seasonal streamflow regime (the hydrograph is dominated by both a snowmelt peak in spring and a rainfall peak in the fall), streamflow will transition to an almost pure rainfall regime (i.e. the spring snowmelt peak will disappear due to loss of snowpack). Results for mean monthly flow show the same outcome as mean daily flow (Figure 13), and are generally consistent with the broad-scale indicators (Figure 11). For both mean daily and monthly flows, a larger change is projected for the RCP8.5 scenario than for the RCP4.5 scenario.

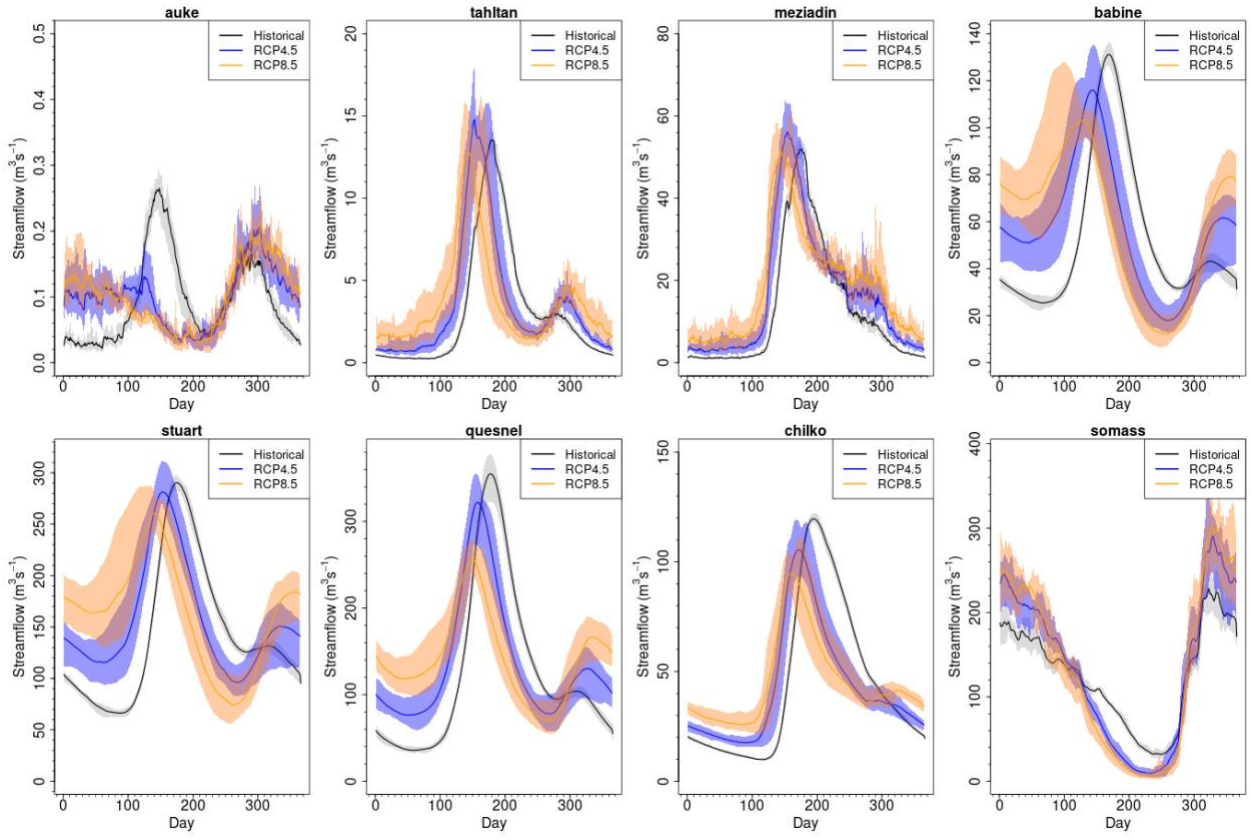

Figure 12. Mean daily flow for the historical (1971-2000) and end-century (2071-2100) periods. Lines represent the ensemble median, and shading shows the ensemble range.

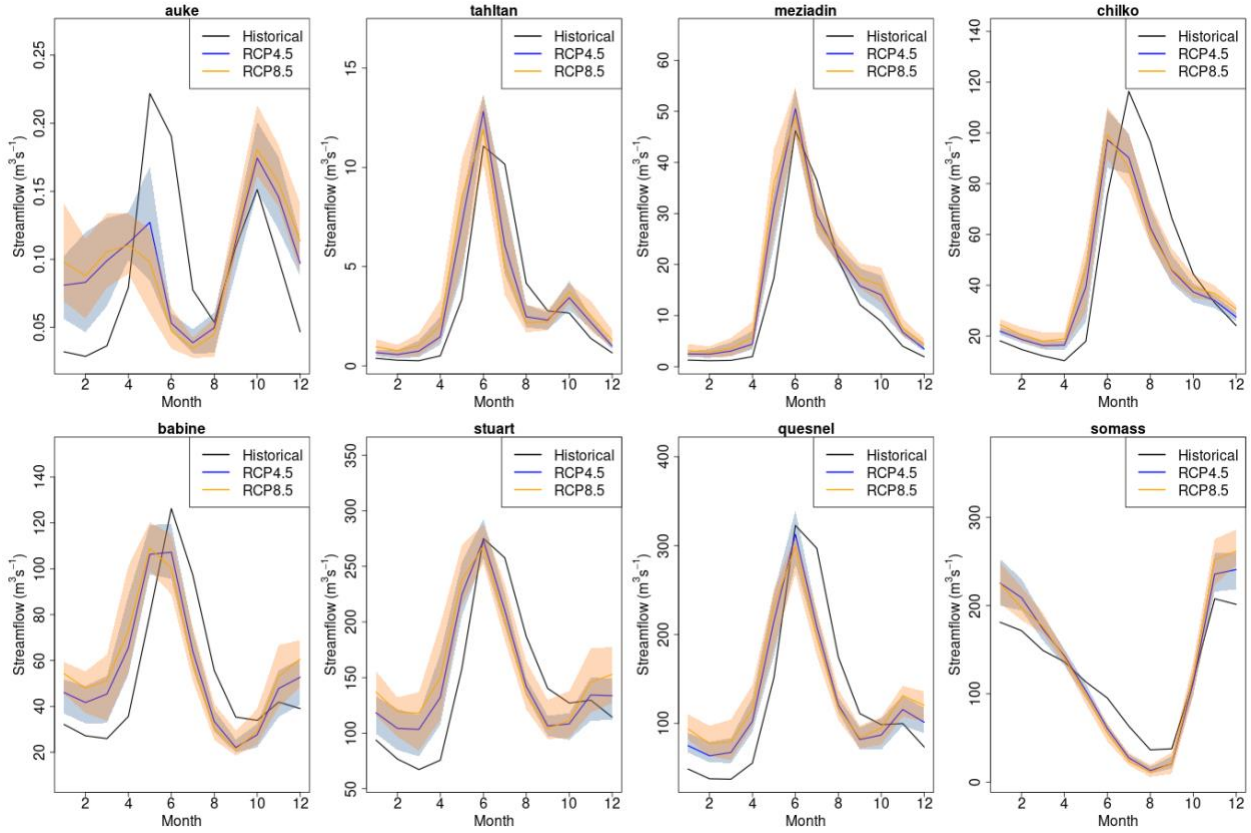

Figure 13. Mean monthly flow for the historical (1971-2000) and end-century (2071-2100) periods. Lines represent the ensemble median and shading shows the ensemble range.

For the frequency of high flow days (days with flow > 95th-percentile historical flow) the response is mixed (Figure 14). The frequency is projected to increase by mid- and end-century in the Tahltan, Meziadin (Surprise) and Somass watersheds. These results are generally consistent with the mean daily and monthly flow indicators (Figure 12 and Figure 13), which show earlier, but larger snowmelt freshets for Tahltan and Meziadin and higher rainfall runoff in the Somass during the late fall. On the other hand, a decrease in the frequency of high flow days is expected in the Auke and Chilko, which is due to the disappearance of the spring snowmelt freshet in the Auke and a decline in the overall magnitude in the peak of the snowmelt freshet in the Chilko (Figure 12). In the remaining watersheds the response is more uncertain. In several cases the ensemble median response is near zero (i.e. no high flow days in future), but a large proportion of the ensemble range lies above the historical frequency (i.e. Babine, Stuart, and Quesnel). The response at mid-century shows little difference between RCP4.5 and RCP8.5, although the response for RCP8.5 tends to be larger than RCP4.5 at end-century.

At most sites, the frequency of low flow days (days with flow < 5th-percentile historical flow) is expected to decrease by mid- and end-century, to the extent that essentially zero low flow days are expected in the future (Figure 15). This is again consistent with the mean daily and monthly flow indicators (Figure 12 and Figure 13). Two exceptions, however, are the Babine and Somass. At both sites the number of low flow days is expected to increase dramatically due to a projected drop in summer discharge.

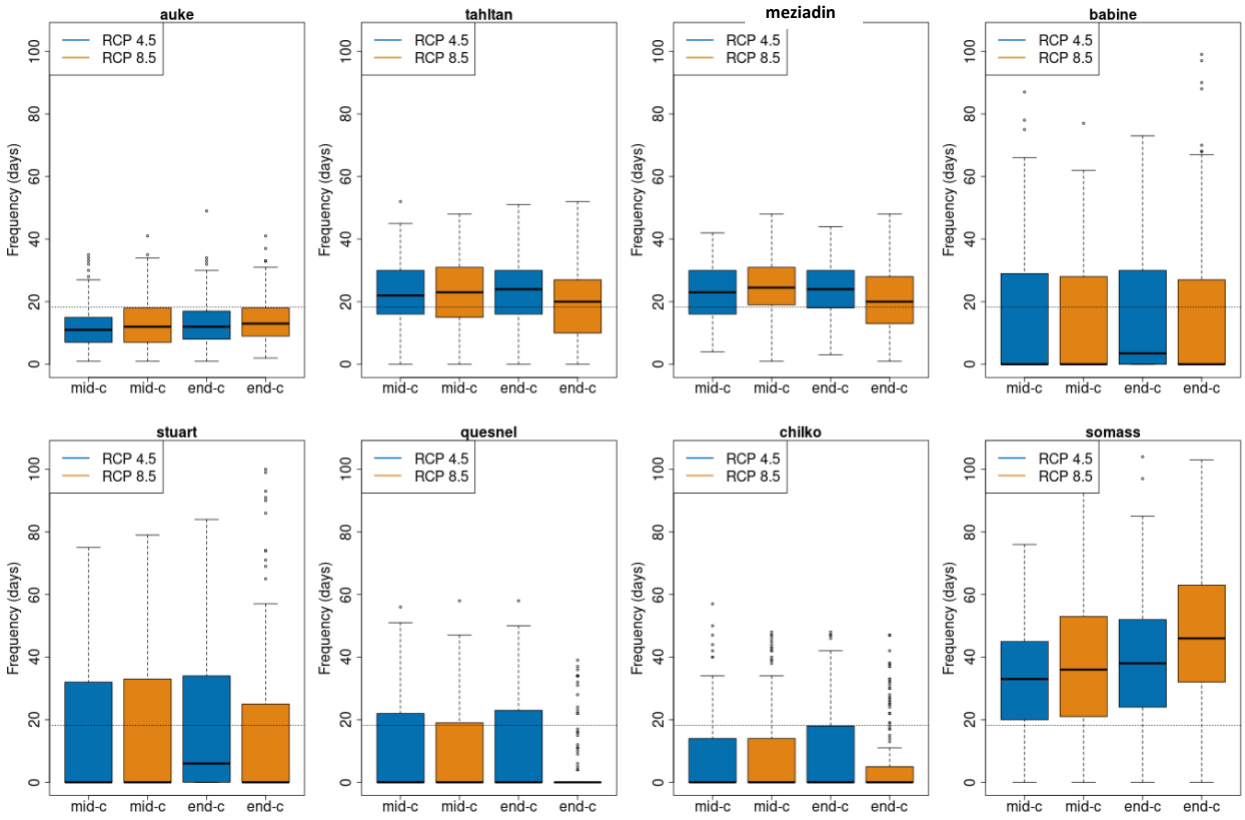

Figure 14. Annual frequency of high flow days (days with flow > 95th-percentile of historical flow) for mid-century and end-century. The baseline value of 18.25 days is indicated by the horizontal line. For the box plots the horizontal line indicates the ensemble median, the box spans the 25th- to 75th-percentile, the whiskers extend to the most extreme data point which is no more than 1.5 times the interquartile range from the box, and the points represent individual outliers. The sample for each box is based on individual annual values for all *PCIC6* models by scenario and period (*N* = 360).

For mean daily water temperature there is a clear signal of increased temperature by end-century at all locations (Figure 16). Both emissions scenarios will experience increased water temperature, although the response for the RCP8.5 scenario is expected to be larger. Water temperature is projected to be larger than historical throughout the year, and the ensemble upper range will approach (Stuart, Tahltan, Meziadin), or exceed (Quesnel and Somass) 30°C in summer by end-century. We note an issue with the data that is apparent on the plots of mean daily water temperature. For several sites (Auke, Tahltan, Meziadin, and to some degree, Babine, and Stuart) spurious jumps and transitions occur. These jumps line up with month boundaries and have been diagnosed as an artefact in the statistically downscaled air temperature, which is applied monthly. This issue affects only the northern portion of the domain. Since the air2stream water temperature model is forced by the downscaled air temperature, this artefact is passed directly to the water temperature projections. Results for mean monthly water temperature (Figure 18) are consistent with those for mean daily water temperature, although the jump artefacts have been removed by the temporal smoothing.

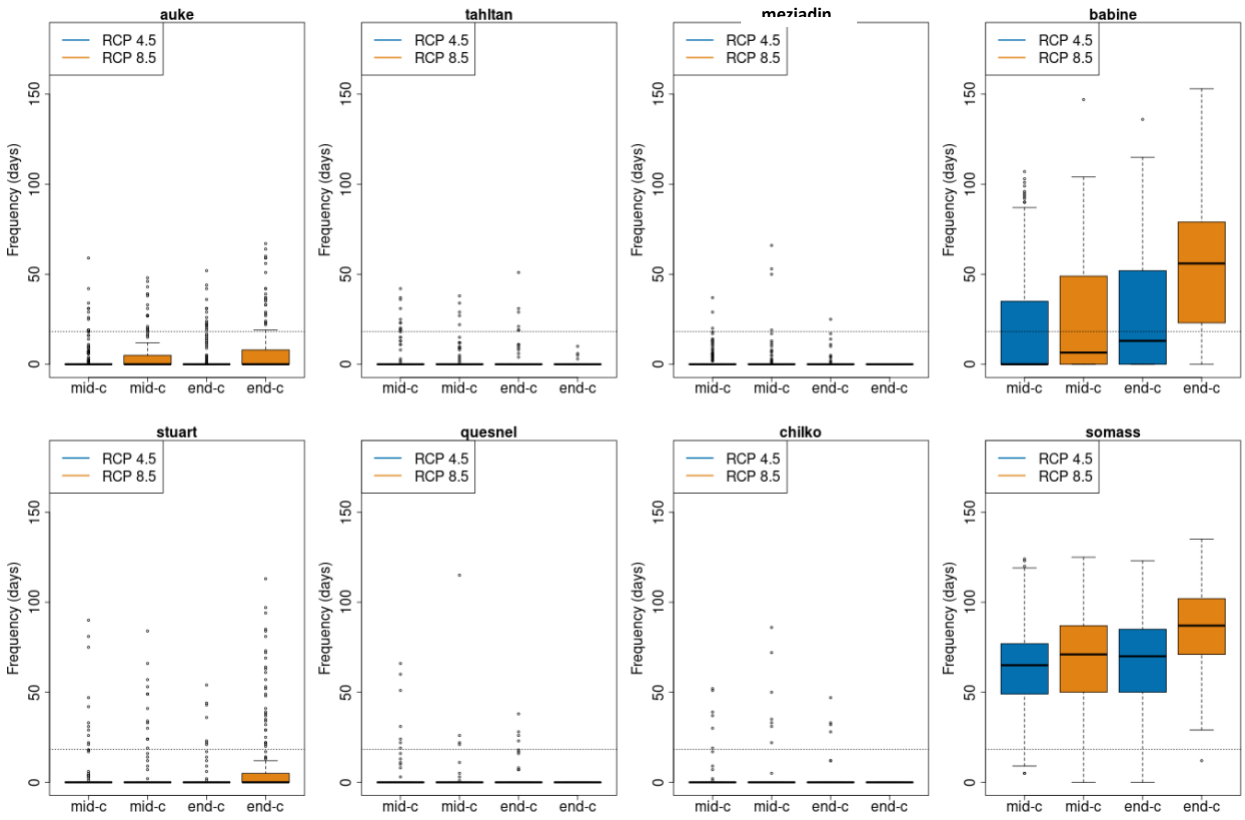

Figure 15. Box-plots of the annual frequency of low flow days (days with flow < 5th-percentile of historical flow) for mid-century and end-century. The baseline value of 18.25 days is indicated by the horizontal line. For the box plots the horizontal line indicates the ensemble median, the box spans the 25th- to 75th-percentile, the whiskers extend to the most extreme data point which is no more than 1.5 times the interquartile range from the box, and the points represent individual outliers. The sample for each box is based on individual annual values for all PCIC6 models by scenario and period (*N* = 360).

Consistent with the general warming trends evident in the mean daily and monthly water temperature, the frequency of days with water temperature more than 19°C is also projected to increase (Figure 18). For all sites the historical frequency is at or near zero, and for most sites (except Chilko) the frequency will increase steadily with increasing warming. At mid-century ensemble median frequencies are expected to range from ~5 days (Babine, RCP4.5) to as high as ~130 days (Somass, RCP8.5). By end century these values are projected to be ~10 days (Babine, RCP4.5) to ~150 days (Somass, RCP8.5). Frequencies increase much more rapidly for RCP8.5 than for RCP4.5, and for any period and site, frequencies for RCP8.5 are roughly double those for RCP4.5. Only discharge form Chilko Lake appears to be somewhat resilient to warming, with frequencies expected to remain near zero mid-century (for both scenarios) and at end-century, but for RCP4.5 only. Even for RCP8.5, the projected frequency at end-century will have an ensemble range of only 2 to 22 days. However, it is possible that the temperature response in the Chilko is underestimated due to the empirical nature of the air2water model? Glacier cover during the historical period makes up 7% of the Chilko watershed, such that air2water is calibrated to historical water temperatures that are presumably cooled by glacier runoff. However, although extrapolation of air2water into the future will account for increasing air temperature, it may not

adequately account for the additional warming that may arise due to the reduction in glacier melt contributions by mid- and end-century.

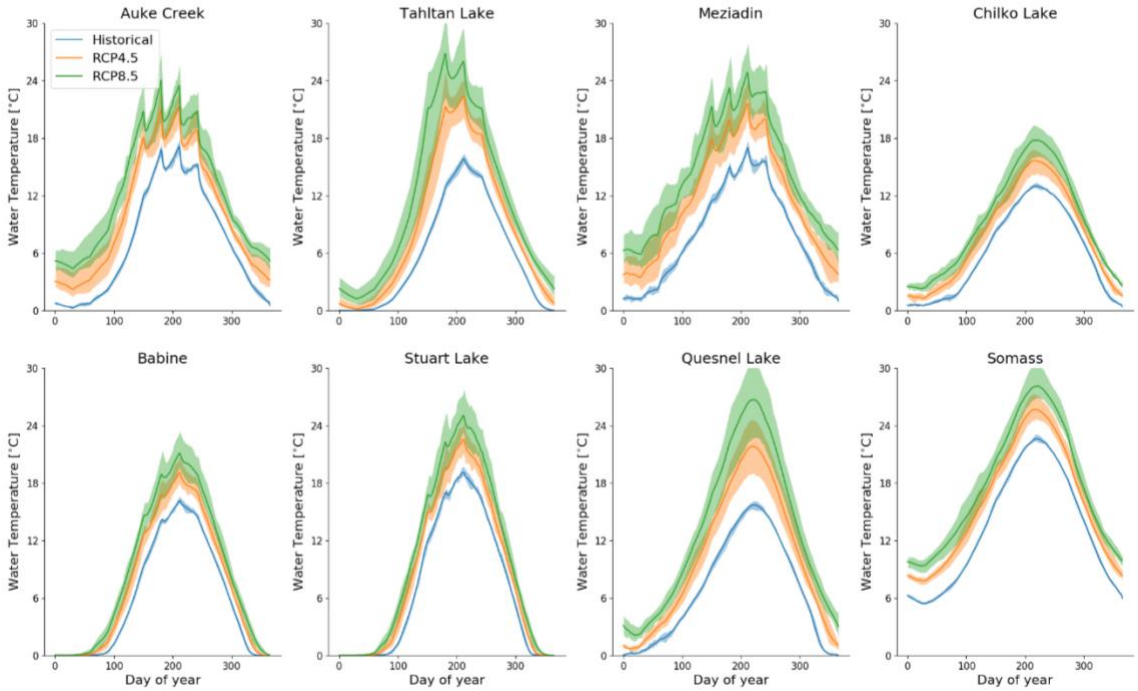

Figure 16. Mean daily water temperature climatology for the historical (1971-2000) and end-century (2071-2100) periods. Lines represent the ensemble median, and shading shows the ensemble range.

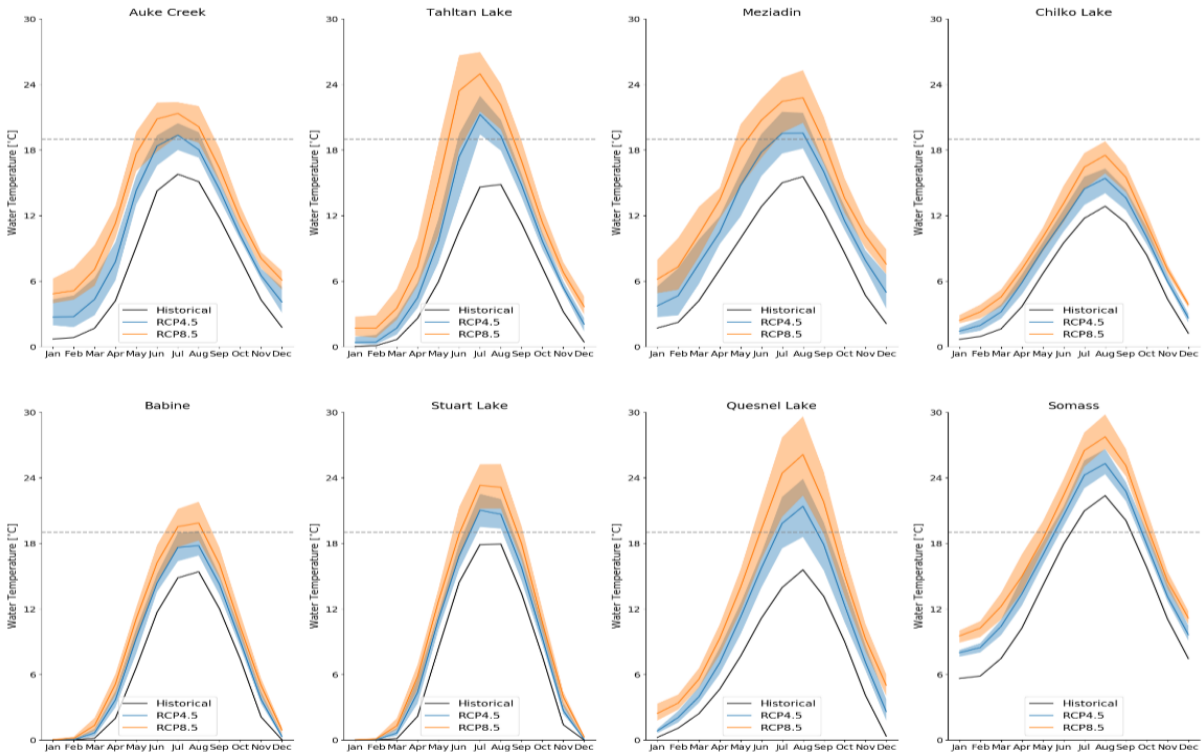

Figure 17. Mean monthly water temperature climatology for the historical (1971-2000) and end-century (2071-2100) periods. Lines represent the ensemble median, and shading shows the ensemble range.

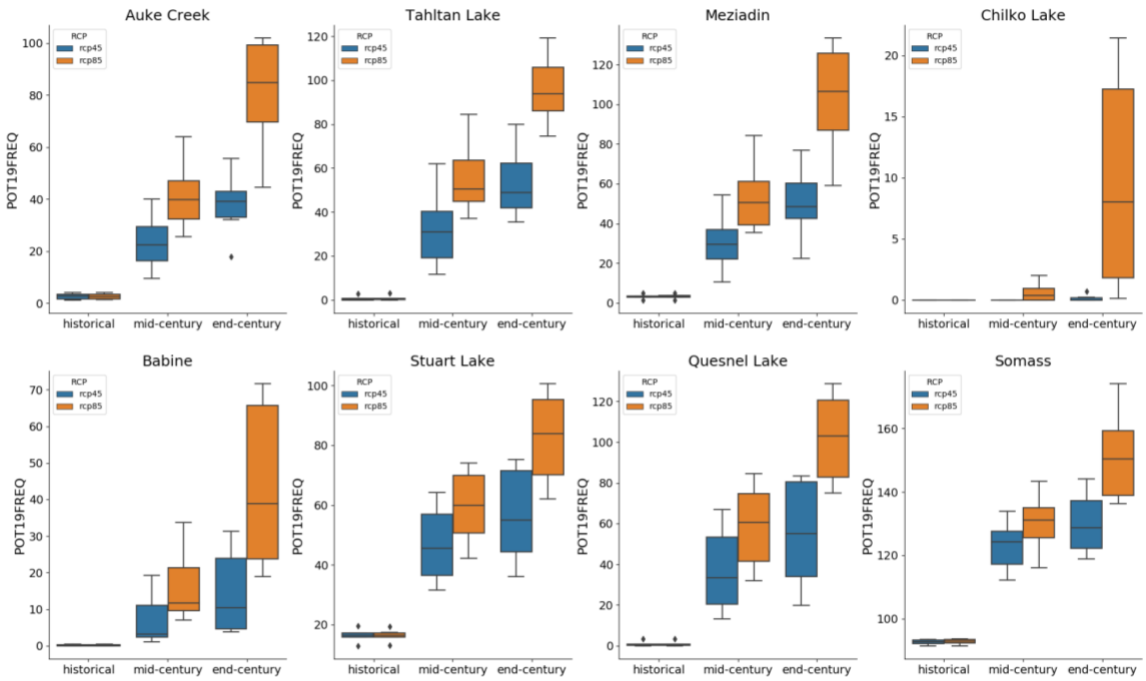

Figure 18. Annual frequency (total days) of water temperature > 19°C for the historical period (1971-2000), mid-century (2041-2070, and end-century (2071-2100). For the box plots the horizontal line indicates the ensemble median, the box spans the 25th- to 75th-percentile, the whiskers show the whiskers extend to the most extreme data point which is no more than 1.5 times the interquartile range from the box, and the points represent individual outliers. The sample for each box is based on individual annual values for all *PCIC6* models by scenario and period (*N* = 360). Note the difference in y-axis range between the panels.

5 The Salmon Climate Impacts Portal

5.1 Description

PCIC's Salmon Climate Impacts Portal (SCIP) is an interactive web application that runs in a user's web browser. It is a tool that has been developed to enables uses to locate, visualize, summarise, and download summary data describing projected changes to flow and thermal hazards in the freshwater environment within the BC Coastal domain. Data is in the form of the gridded broad-scale indicators (Section 4.1) describing a range of streamflow and water temperature hazards over annual, monthly, and daily time scales. The SCIP uses the broad scale hazard indicators produced with the *PCIC6-full* ensemble (3.1). The data in the SCIP uses only the climatological mean values for each individual climate run (i.e. the climatological minimum, maximum, and standard deviations are not currently used).

The SCIP provides visualizations in the form of maps and regional summaries in the form of graphs. Specifically, the SCIP is to allow users to:

- Select data from six global climate models, two greenhouse gas concentration scenarios, and ten hazard indices.
- Select a specific time horizon (1971-2000, 2011-2040, 2041-2070, 2071-2100).
- Visualize maps of gridded hazard indices.
- Generate summary plots by region of interest.
- Select region of interest by watershed group, salmon conservation unit or custom outlet location.
- Download summary data.

This tool is primarily designed to serve the needs of technical and scientific users who require climate change information for salmon environmental impacts and vulnerability studies. However, the tool will also be of interest to the broad range of users involved in fisheries management.

Due to the spatial resolution of the broad-scale gridded data this tool is intended to provide a regional overview of potential changes in freshwater hazards and is not generally recommended for site-specific assessments. Therefore, a region of interest (ROI) must be selected for the purposes of creating a data summary of a chosen indicator. A ROI can be chosen using either pre-defined areas based on watersheds or salmon conservation units, or by manually selecting an outlet point on the map (Figure 19). Watershed regions are based on the watershed groups (defined by the BC Freshwater Atlas (Ministry of Forests, 2024). Only watershed groups for which hazard indicator data is available are listed (currently 118). Users also have the option of defining the ROI based on salmon conservation units (CUs). According to Canada's Policy for Conservation of Wild Pacific Salmon "A Conservation Unit (CU) is a group of wild salmon sufficiently isolated from other groups that, if extirpated, is very unlikely to recolonize naturally within an acceptable timeframe, such as a human lifetime or a specified number of salmon generations" (Fisheries and Oceans Canada, 2005). Only CUs for which hazard indicator data is available are listed (currently 114 CUs).

Access to the SCIP is via the following link: https://services.pacificclimate.org/scip/app/

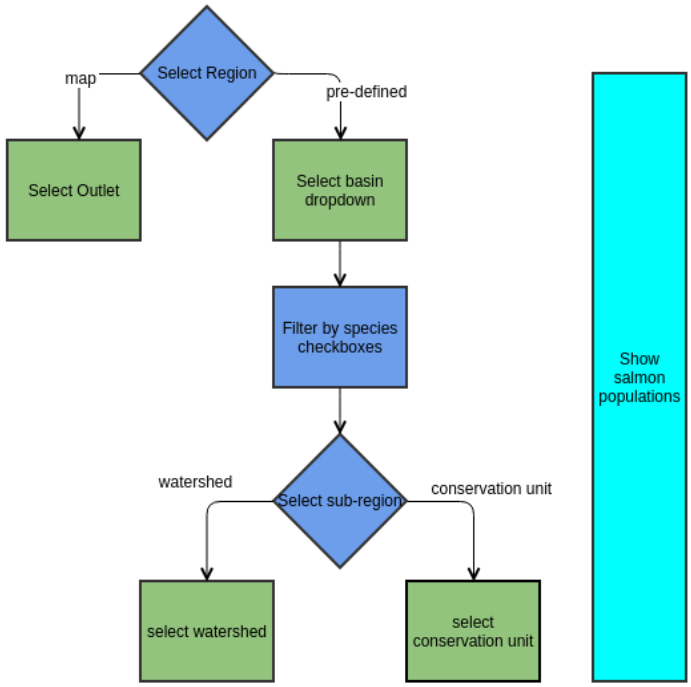

Figure 19. Schematic of the region selection process

5.2 Data Portal Components

The architecture of the SCIP strongly leverages open-source software and libraries and makes extensive use of the PCEX API, which is a data server developed from scratch at PCIC that dynamically calculates statistical data from netCDF-formatted files for PCIC web applications. The SCIP is composed of three main components: a website, data servers, and the data, which are described in detail in the following sections.

5.2.1 Website

The website is written in JavaScript using the industry standard open-source toolkits React (https://react.dev/) for user interfaces, Plotly (https://plotly.com/python/) for data visualization, and Leaflet (https://leafletjs.com/) for map display. It brings together data from three PCIC-run data servers to allow the user to summarize and compare projected hazard indices and data on salmon populations for a selected geographical area of interest. This is the public-facing component of the website that allows users to interactively explore and summarise the hazard indicator data.

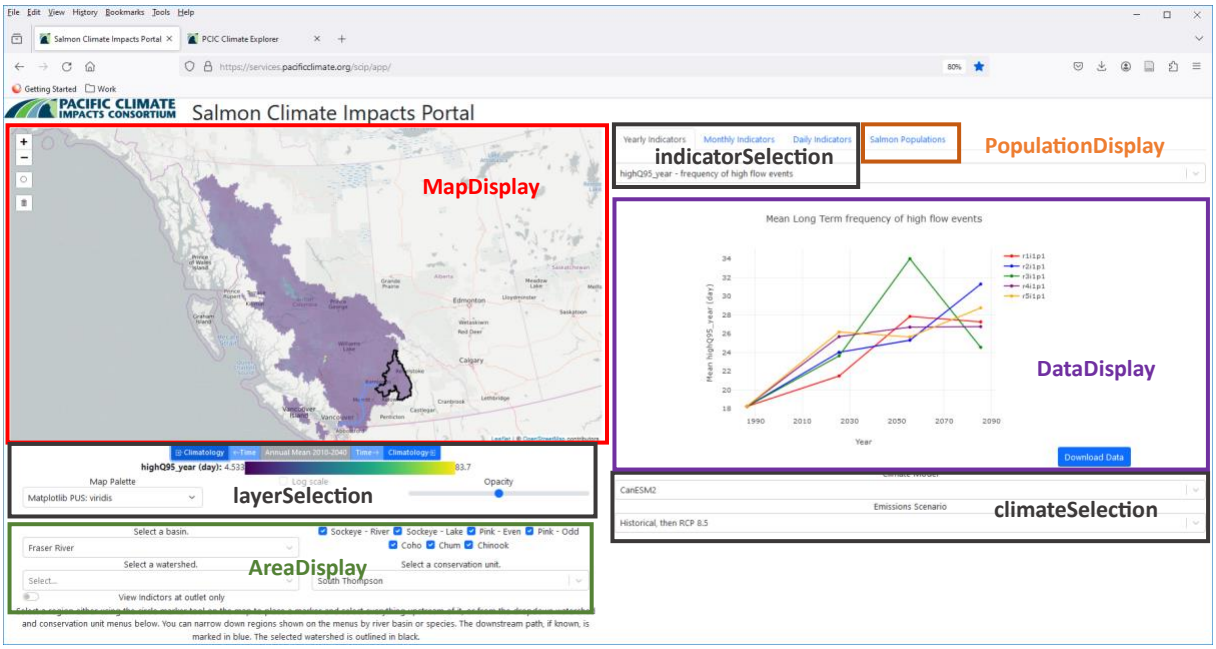

Figure 20. Screen capture of Salmon Climate Impacts Portal website showing the main website components.

The layout of the website is shown in Figure 20, and the four main components (Figure 21) of the website are as follows:

2. The **MapDisplay** is an interactive web map that presents the datasets selected from the filtered collection (red box in Figure 20). It shows a spatial slice of the data for a specific point in time. A single index is represented as a raster (a grid of coloured blocks) overlaid on the base map. Colours encode the variable's value. The data map is the most complex data presentation tool and has a small collection of generic web mapping features and data presentation features (Figure 22).

3. The **DataDisplay** presents a non-spatial view of a dataset (purple box in Figure 20). This view is temporal, that is, it is a graph with time as the horizontal axis. This data graph presents a summary of a filtered collection of datasets for a selected region of interest either as a spatial average or, if preferred, by showing results for the outlet cell of the selected region. Charts differ slightly depending on the temporal resolution of the indicator. For annual indicators individual datasets within a filtered collection are plotted by model run, and climatological period (Figure 23). For monthly and daily indicators datasets are also plotted by time step (see Figure 24 and Figure 25 for monthly and daily resolution, respectively).

4. The **Area Display** shows information about available watersheds or conservation units (green box in Figure 20). The AreaDisplay contains a set of selection tools that are used to select a region of interest (ROI) for the purposes of creating a data summary of a chosen hazard indicator. A ROI can be chosen using either pre-defined areas based on watershed groups or salmon conservation units (where the choice of available CU's can be filtered by salmon species),

or by manually selecting an outlet point on the map. The tool for custom selection is in the **MapDisplay**.

5. The **PopulationDisplay** lists all salmon populations within a user-selected area, by species, or subspecies, and conservation unit name and code. Population data is displayed in tabular format and accessed via the Salmon Population table (see orange box in Figure 20).

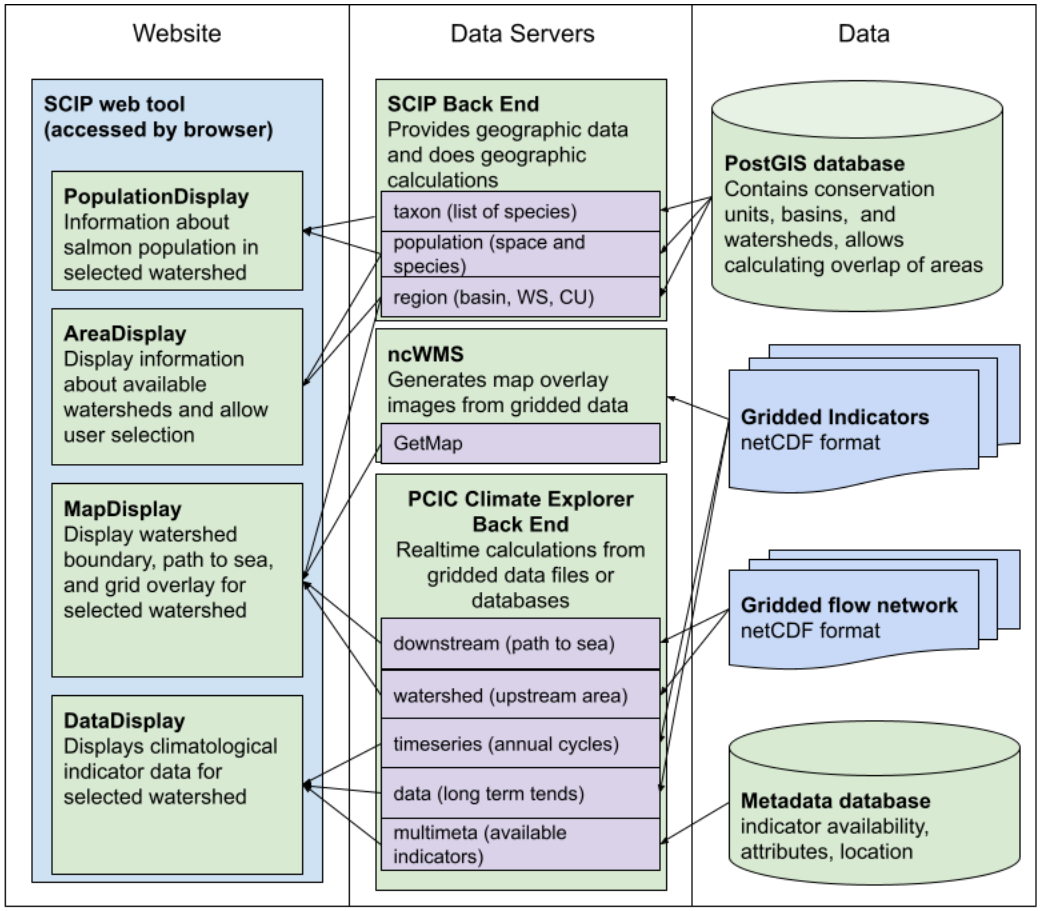

Figure 21. Components of the Salmon Climate Impacts Portal

The website also contains a set of selection tools for data set selection and filtering.

1. The **indicatorSelection** and **climateSelection** filter the data into a collection of multiple *datasets*. This collection of datasets contains indicator values for multiple model runs (for GCMs with multiple runs), all four climatological periods and, for monthly and daily indicators, multiple time steps. Additional dataset discrimination is available in the **MapDisplay** and **DataDisplay**.
2. The **layerSelection** tools can be used to change the dataset layer viewed in the **MapDisplay**. The ***climatology*** buttons move through the four different climatology periods. For monthly and daily

indicators, the ***time*** buttons advance through the months (January through December) and days of the year (1 January through 31 December), respectively.

5.2.2 Data Servers

The data servers access, summarize, and format data for the website's needs in real-time. The following data servers are utilized (Figure 21):

1. **SCIP Back End** is a geospatial data server designed from the ground up to support the multiple spatial frameworks needed by the website. It provides an interface between the website and a PostGIS spatial database (https://postgis.net) to do spatial calculations. The following APIs are available:
    - taxon – provides data about salmon species and subspecies
    - population – return data about salmon populations (species, location)
    - region – return information on named pre-defined regions (drainage basins, watersheds, salmon conservation units) fitting supplied parameters
2. **ncWMS** is an open-source geospatial data server (https://reading-escience-centre.github.io/ncwms/). It reads gridded quantitative data from a netCDF dataset, such as indicator data, and translates it into colour-coded map images, which the website front end displays as part of the interactive map.
3. The **PCIC Climate Explorer Back End** is used by several PCIC tools to calculate summary data suitable for web display from a combination of netCDF files and postGIS databases. The SCIP website uses both pre-existing APIs for calculating climatological time series and the following newly developed APIs that provide the hydrological data inputs needed by this tool:
    - modelmeta - informs the website which indicators and data files are available.
    - timeseries - calculates the average daily or monthly cycle of an indicator over the course of a year.
    - data - calculates the long-term change in the average value of an indicator.
    - downstream - calculates the downstream route toward the sea from a point.
    - watershed - calculates the upstream drainage area from a point.

5.2.3 Data

Data (Figure 21; Table 6) are stored, in various formats, on redundant PCIC systems and formatted for ease of use by the website by data servers in real-time as needed. This approach offers flexibility in what questions our data can be used to answer and makes it easy to update or correct data as new data is created.

Table 6. Data Files

Data	Format	Source	Spatial Extent
Watersheds	PostGIS database	BC Freshwater Atlas Watershed Groups (GeoBC, 2011)	Pacific (Figure 2)
Salmon Conservation Units	PostGIS database	Pacific salmon conservation units (Fisheries and Oceans Canada, 2017).	Pacific (Figure 2)
Flow networks	Gridded netCDF	Dominant River Tracing (DRT) product (Wu et al., 2012)	Pacific (Figure 2)
Indicators	Gridded netCDF	This project (broad-scale hydrologic modelling)	VIC-GL domain (Figure 2)
Data file metadata	Postgres database	This project (broad-scale hydrologic modelling)	n/a

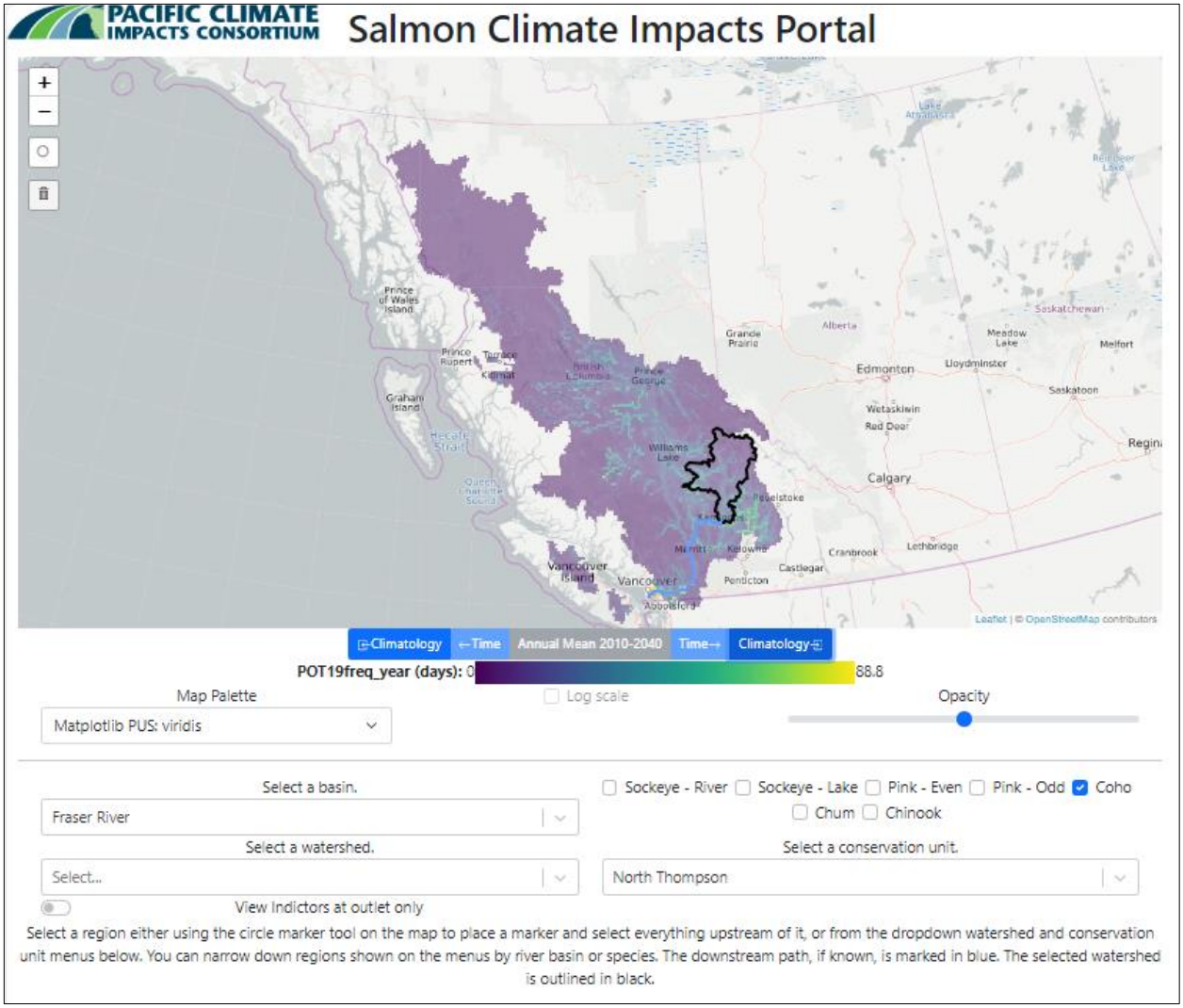

Figure 22. Screen capture of SCIP website showing map display, layer display tools, and region selection tools. The data layer shown in the map is *POT19freq_year* for the 2010-2040 for the CCSM4 GCM and emissions scenario RCP8.5 and the region selected is Coho conservation unit 'North Thompson'.

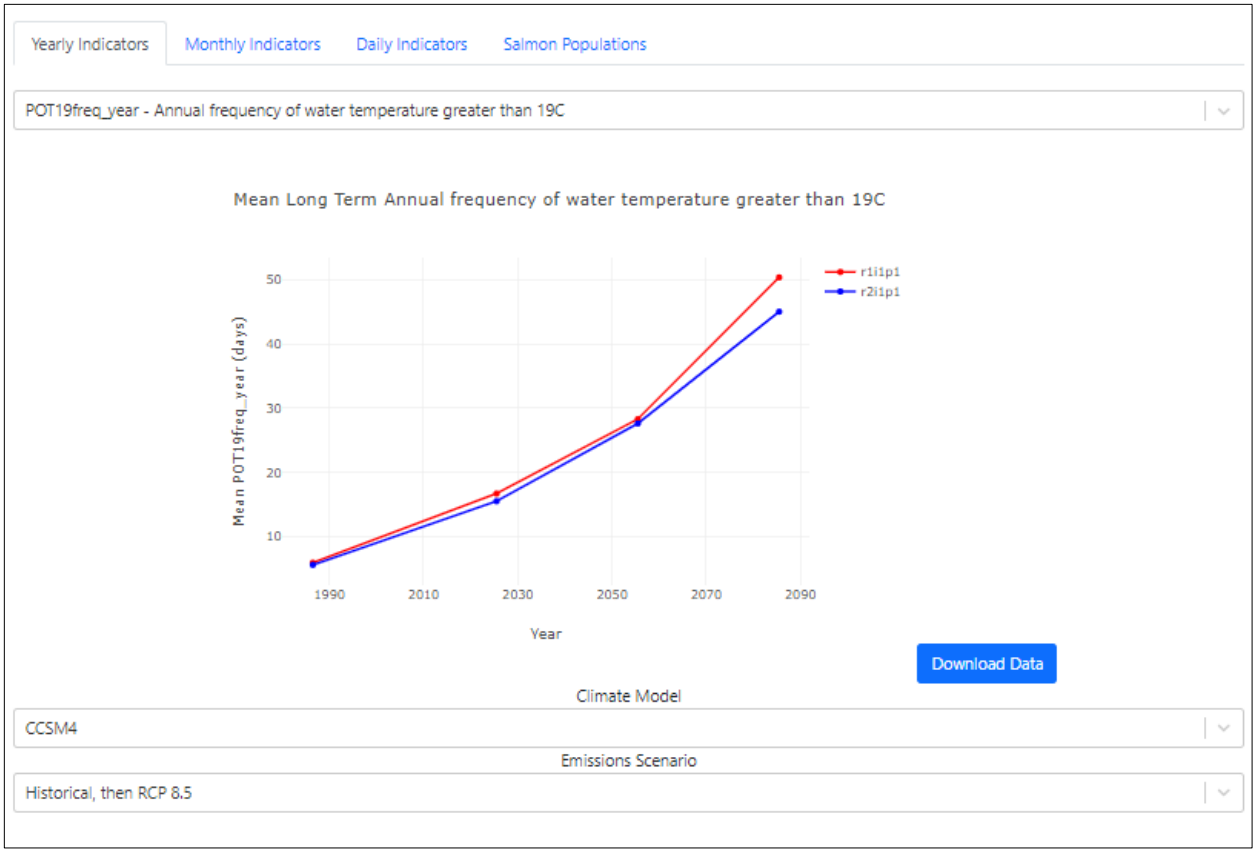

Figure 23. Screen capture of SCIP website showing data selection tools and summary data display. In this example the data summary is for *POT19freq_year* for the CCSM4 GCM and emissions scenario RCP8.5 for the Coho conservation unit 'North Thompson'. A curve of *POT19freq_year* versus climate period is plotted for each run (r1i1p1 and r2i2p2) of the CCSM4 GCM.

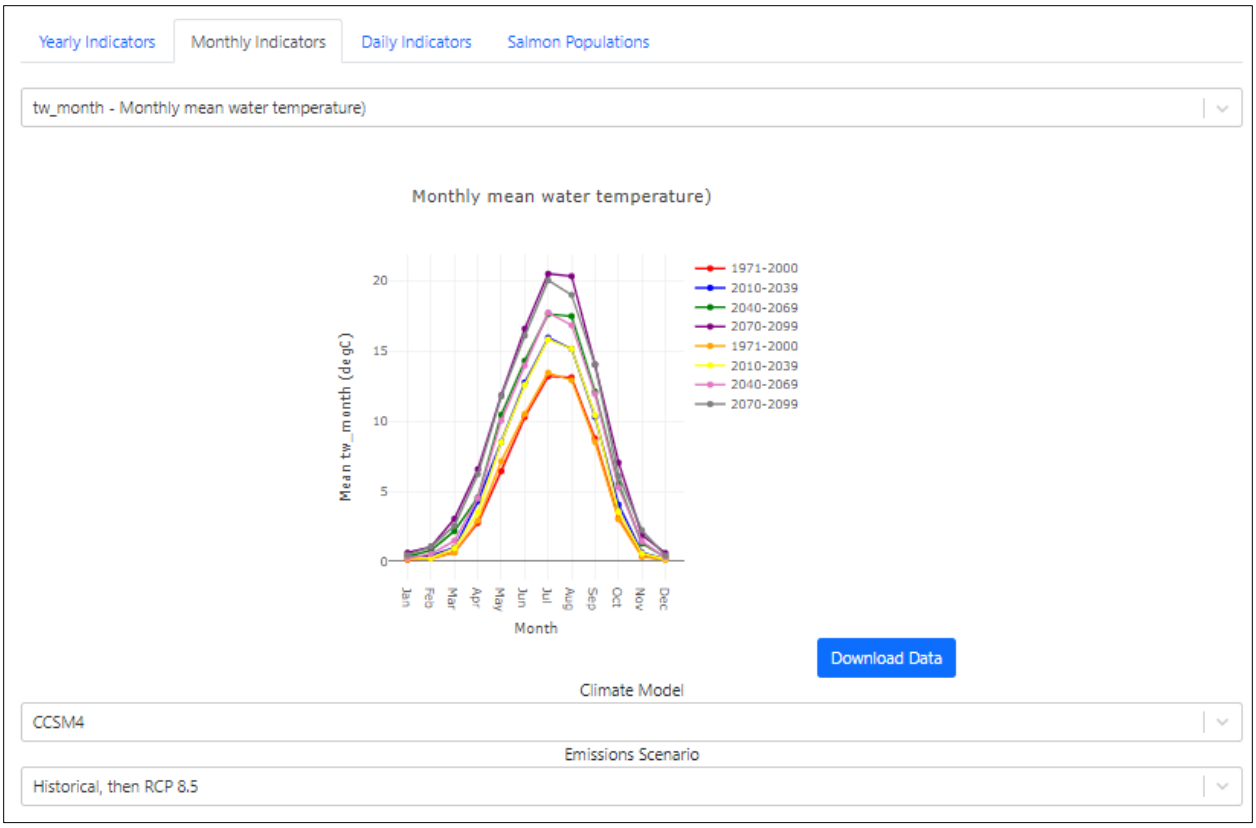

Figure 24. Screen capture of SCIP website showing data selection tools and data summary graph display. The data summary is for monthly mean water temperature (*tw_month*) for the CCSM4 GCM and emissions scenario RCP8.5 for the Coho conservation unit 'North Thompson'. A curve of *tw_month* versus month is plotted for each run (r1i1p1 and r2i2p2) of the CCSM4 GCM and each climate period.

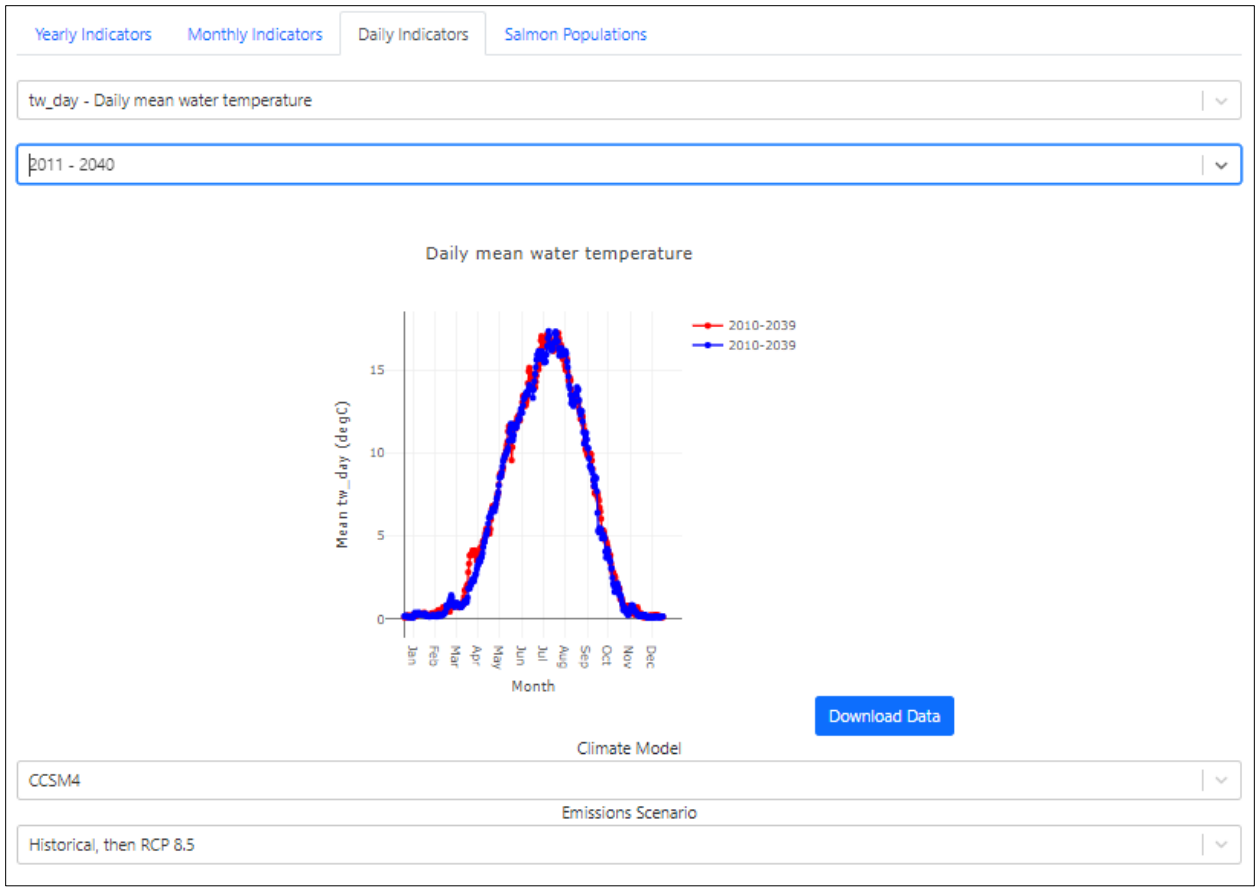

Figure 25. Screen capture of SCIP showing data selection tools and data summary graph display. The data summary is for daily mean water temperature (*tw_day*) for the CCSM4 GCM, emissions scenario RCP8.5, and period 2011-2040 for the Coho conservation unit 'North Thompson'. A curve of *tw_day* versus day of year is plotted for each run (r1i1p1 and r2i2p2) of the CCSM4 GCM.

6 Data Availability

Although not the specific goal of this project, the hydrologic projections used to derive the freshwater hazard indicators are an important product in and of themselves. The raw streamflow and water temperature projections could be used by advances users to develop and explore more customized indicators than those currently available, such as such as cumulative degree-days for a specific period, alternative flow and temperature thresholds, or different temporal scales (such as weekly), etc. In this way, users can produce hazard data tailored to a specific species, population and/or freshwater life stage (e.g. smoltification, adult or juvenile migration, spawning). Users can also use the available gridded indicators to develop assessment for specific regions not currently available in the SCIP. The streamflow and water temperature projections for the fine-scale study sites can be used in the same fashion for the relevant indicator stocks. The raw hydrologic projections can also be used to assess hydrologic impacts due to climate change more broadly, not just as it specifically pertains to salmon freshwater hazard.

Data availability is summarised in Table 7. Due to the size of the dataset the broad-scale and fine-scale streamflow and water temperature projections are not currently accessible via an online tool, but this data resides on the redundant PCIC storage system and can be made available upon request to the project Principal Investigator (PI), Markus Schnorbus (mschnorb@uvic.ca). The broad scale indicators (climatological means only) have been deployed to the SCIP (see Section 5), where users will be able to visualize and download summary data. Although the raw gridded indicator data can be viewed in the SCIP (via the map viewer), there is yet no means to directly download the raw indicator data. However, this data can also be made available by contacting the aforementioned project PI. Fine-scale streamflow and water temperature projections, and associated indicators, are also available upon request for all the sites listed in Table 4.

Table 7. Data availability

Scale	Data	Format	Availability	Ensemble
Broad scale	Streamflow projections	Grided netCDF	Upon request	*PCIC6-full* (32 files)
	Water temperature projections	Grided netCDF	Upon request	*PCIC6-full* (32 files)
	Hazard indicators	Grided netCDF	Raw data upon request; visualization and summary data of climatological means available through SCIP	*PCIC6-full* (5120 files)
Fine scale	Streamflow projections	Text files	Upon request	*PCIC6* (132 files)
	Water temperature projections	Text files	Upon request	*PCIC6* (132 files)
	Hazard indicators	Text files	Upon request	*PCIC6*

7 Conclusion

PCIC has completed a project to quantify freshwater hazards for salmon populations throughout the Pacific Region of British Columbia. Flow and thermal indicators have been produced that capture and quantify historical and potential future freshwater hazards over a large spatial domain and at multiple temporal scales (daily, weekly, monthly, and seasonally). This knowledge is delivered to a broad range of users via the Salmon Climate Impacts Portal (SCIP). This data, and associated tool, will support assessments of ecological vulnerability to climate change across diverse salmon habitats and populations. The chosen indicators are intended to be somewhat generic and, therefore, applicable across a broad region and a wide range of salmon populations. Although the selected indicators will not satisfy the specific needs of all users, they should provide a solid regional overview of the range of freshwater hazards encountered by salmon both historically and under the impact of future climate change.

Hazard indicators were calculated from streamflow and water temperature projections driven by an ensemble of climate forcing experiments covering to the end of the current century. Using this design the *PCIC6* ensemble explicitly assesses the uncertainty in future projections due to a range of greenhouse gas emissions and that due to differences between GCMs. The *PCIC6-full* ensemble, with multiple realizations for several GCMs, also assesses additional uncertainty due to internal climate variability. The production of hazard indicators adopted a parallel approach with two 'scales' of assessment: a detailed fine-scale assessment specifically tagged to representative Sockeye and Chinook Salmon indicator stocks in eight watersheds, and a broader-scale regional assessment at coarser resolution along 399400 km^2 area of coastal draining watersheds. Output from the VIC-GL and DynWat models was used for the broad-scale regional analysis of climate change impacts and the Raven hydrologic modelling framework in conjunction with air2water was used to conduct more detailed hydrologic modelling of smaller watersheds for the fine-scale hazard assessment.

The Salmon Climate Impacts Portal (SCIP) is an online tool developed at PCIC to enables uses to locate, visualize, summarise, and download summary data describing projected changes to hazards in the freshwater environment within the BC Coastal domain. It is designed for conducting regional population- and watershed-based summaries based on the broad-scale indicators in support climate change ecological vulnerability assessments. This tool is primarily designed to serve the needs of technical and scientific users who require climate change information for salmon environmental impacts and vulnerability studies. However, the tool will also be of interest to the broad range of users involved in fisheries management. Although not incorporated into the SCIP, the fine-scale hazard indicators are available from PCIC and will provide a valuable resource for any future vulnerability assessments of the relevant indicator stocks.

8 References

Arora, V.K., Cannon, A.J., 2018. A brief background on climate models: the source of future climate information. In: P. Mukhopadhyaya (ed.), 1st International Conference on New Horizons in Green Civil Engineering (NHICE-01), Victoria, BC, Canada, April 25-27, 2018. ISBN: 978-1-55058-620-6. p. 348-356.

Babaluk, J.A., Reist, J.D., Johnson, J.D., Johnson, L., 2000. First records of sockeye (Oncorhynchus nerka) and pink salmon (O. gorbuscha) from Banks Island and other records of Pacific salmon in Northwest Territories, Canada. Arctic 53, 161–164. https://doi.org/10.14430/arctic846

Baret, F., Weiss, M., Lacaze, R., Camacho, F., Makhmara, H., Pacholcyzk, P., Smets, B., 2013. GEOV1: LAI and FAPAR essential climate variables and FCOVER global time series capitalizing over existing products. Part1: Principles of development and production. Remote Sensing of Environment 137, 299–309. https://doi.org/10.1016/j.rse.2012.12.027

Battin, J., Wiley, M.W., Ruckelshaus, M.H., Palmer, R.N., Korb, E., Bartz, K.K., Imaki, H., 2007. Projected impacts of climate change on salmon habitat restoration. PNAS 104, 6720–6725. https://doi.org/10.1073/pnas.0701685104

Beechie, T., Buhle, E., Ruckelshaus, M., Fullerton, A., Holsinger, L., 2006. Hydrologic regime and the conservation of salmon life history diversity. Biological Conservation 130, 560–572. https://doi.org/10.1016/j.biocon.2006.01.019

Bos, M.G. (Ed.), 1989. Discharge measurement structures, Third revised edition. ed, ILRI publication. International Institute for Land Reclamation and Improvement (ILRI), Wageningen, The Netherlands.

Camacho, F., Cernicharo, J., Lacaze, R., Baret, F., Weiss, M., 2013. GEOV1: LAI, FAPAR essential climate variables and FCOVER global time series capitalizing over existing products. Part 2: Validation and intercomparison with reference products. Remote Sensing of Environment 137, 310–329. https://doi.org/10.1016/j.rse.2013.02.030

Cannon, A.J., 2015. Selecting GCM Scenarios that Span the Range of Changes in a Multimodel Ensemble: Application to CMIP5 Climate Extremes Indices. J. Climate 28, 1260–1267. https://doi.org/10.1175/JCLI-D-14-00636.1

Cannon, A.J., Jeong, D.I., Zhang, X., Zwiers, F.W., 2020. , in: Chapter 2 in CLIMATE-RESILIENT BUILDINGS & CORE PUBLIC INFRASTRUCTURE: An Assessment of the Impact of Climate Change on Climatic Design Data in Canada. Environment and Climate Change Canada. DRAFT. Victoria, BC, Canada, p. 15 pp.

Cannon, A.J., Sobie, S.R., Murdock, T.Q., 2015. Bias Correction of GCM Precipitation by Quantile Mapping: How Well Do Methods Preserve Changes in Quantiles and Extremes? Journal of Climate 28, 6938–6959. https://doi.org/10.1175/JCLI-D-14-00754.1

Caretta, M.A., Mukherji, A., Arfanuzzaman, M., Betts, R.A., Gelfan, A., Hirabayashi, Y., Lissner, T.K., Liu, J., Gunn, E.L., Morgan, R., Mwanga, S., Supratid, S., 2022. Water, in: Pörtner, H.-O., Roberts, D.C., Tignor, M., Poloczanska, E.S., Mintenbeck, K., Alegría, A., Craig, M., Langsdorf, S., Löschke, S., Möller, V., Okem, A., Rama, B. (Eds.), Climate Change 2022: Impacts, Adaptation, and Vulnerability. Contribution of Working Group II to the Sixth Assessment Report of the Intergovernmental Panel on Climate Change. Cambridge University Press.

Carothers, C., Sformo, T.L., Cotton, S., George, J.C., Westley, P.A.H., 2019. Pacific salmon in the rapidly changing arctic: Exploring local knowledge and emerging fisheries in Utqiaġvik and Nuiqsut, Alaska. Arctic 72, 273–288. https://doi.org/10.14430/arctic68876

Cherkauer, K.A., Bowling, L.C., Lettenmaier, D.P., 2003. Variable infiltration capacity cold land process model updates. Global and Planetary Change 38, 151–159.

Chila, Z.K.E., Dunmall, K., Proverbs, T., Lantz, T., Hunters and Trappers Committee, A., Hunters and Trappers Committee, I., Hunters and Trappers Committee, S.H., Hunters and Trappers Committee, O., Hunters and Trappers Committee, P., 2021. Inuvialuit Knowledge of Pacific Salmon Range Expansion in the Western Canadian Arctic. Canadian Journal of Fisheries and Aquatic Sciences 1–52. https://doi.org/10.1139/cjfas-2021-0172

Craig, J.R., Brown, G., Chlumsky, R., Jenkinson, R.W., Jost, G., Lee, K., Mai, J., Serrer, M., Sgro, N., Shafii, M., Snowdon, A.P., Tolson, B.A., 2020. Flexible watershed simulation with the Raven hydrological modelling framework. Environmental Modelling & Software 129, 104728. https://doi.org/10.1016/j.envsoft.2020.104728

Crossin, G.T., Hinch, S.G., Cooke, S.J., Welch, D.W., Patterson, D.A., Jones, S.R. m., Lotto, A.G., Leggatt, R.A., Mathes, M.T., Shrimpton, J.M., Van Der Kraak, G., Farrell, A.P., 2008. Exposure to high temperature influences the behaviour, physiology, and survival of sockeye salmon during spawning migration. Can. J. Zool. 86, 127–140. https://doi.org/10.1139/Z07-122

Crozier, L.G., McClure, M.M., Beechie, T., Bograd, S.J., Boughton, D.A., Carr, M., Cooney, T.D., Dunham, J.B., Greene, C.M., Haltuch, M.A., Hazen, E.L., Holzer, D.M., Huff, D.D., Johnson, R.C., Jordan, C.E., Kaplan, I.C., Lindley, S.T., Mantua, N.J., Moyle, P.B., Myers, J.M., Nelson, M.W., Spence, B.C., Weitkamp, L.A., Williams, T.H., Willis-Norton, E., 2019. Climate vulnerability assessment for Pacific salmon and steelhead in the California Current Large Marine Ecosystem. PLOS ONE 14, e0217711. https://doi.org/10.1371/journal.pone.0217711

Crozier, L.G., Siegel, J.E., Wiesebron, L.E., Trujillo, E.M., Burke, B.J., Sandford, B.P., Widener, D.L., 2020. Snake River sockeye and Chinook salmon in a changing climate: Implications for upstream migration survival during recent extreme and future climates. PLOS ONE 15, e0238886. https://doi.org/10.1371/journal.pone.0238886

Danielson, J.J., Gesch, D.B., 2011. Global Multi-resolution Terrain Elevation Data 2010 (GMTED2010). U.S. Geological Survey Open-File Report 2011–1073. U.S. Department of the Interior, U.S. Geological Survey, National Geospatial-Intelligence Agency.

Demarchi, D.A., 2011. An Introduction to the Ecoregions of British Columbia. Victoria, BC.

Dingman, S.L., 2015. Physical Hydrology, Third. ed. Waveland Press, Inc., Long Grove, Illinois.

Dorner, B., Catalano, M.J., Peterman, R.M., 2017. Spatial and temporal patterns of covariation in productivity of Chinook salmon populations of the northeastern Pacific Ocean. Can. J. Fish. Aquat. Sci. 75, 1082–1095. https://doi.org/10.1139/cjfas-2017-0197

FAO, 2015. Assessing climate change vulnerability in fisheries and aquaculture: Available methodologies and their relevance for the sector, FAO Fisheries and Aquaculture Technical Paper. Food and Agricultural Organization of the United Nations, Rome, Italy.

Fisheries and Oceans Canada, 2017. Pacific Salmon Conservation Units, Sites & Status - Open Government Portal [WWW Document]. URL https://open.canada.ca/data/en/dataset/1ac00a39-4770-443d-8a6b-9656c06df6a3 (accessed 5.10.24).

Fisheries and Oceans Canada, 2016. Integrated biological status of southern British Columbia Chinook salmon (Oncorhynchus tshawytscha) under the Wild Salmon Policy (Canadian Science Advisory Secretariat, science advisory report No. 2016/042). Fisheries and Oceans Canada, Nanaimo, BC.

Fisheries and Oceans Canada, 2005. Canada's Policy for Conservation of Wild Pacific Salmon. Fisheries and Oceans Canada, Vancouver, BC.

Fread, D.L., 1992. Flow Routing, in: Maidment, D.R. (Ed.), Handbook of Hydrology. McGraw-Hill, Inc., New York, NY, p. Chapter 10.

GeoBC, 2011. Freshwater Atlas Watershed Groups - Datasets - Data Catalogue [WWW Document]. URL https://catalogue.data.gov.bc.ca/dataset/freshwater-atlas-watershed-groups (accessed 5.10.24).

Global Soil Data Task, 2014. Global Soil Data Products CD-ROM Contents (IGBP-DIS). ORNL DAAC, doi:https://doi.org/10.3334/ORNLDAAC/565.

Government of British Columbia, 2024. Bathymetric Maps - Open Government Portal [WWW Document]. URL https://open.canada.ca/data/en/dataset/1427d389-cd21-4fe2-8ed9-282d9bdcb7e2 (accessed 4.11.24).

Gudmundsson, G.H., Krug, J., Durand, G., L., Favier., Gagliardini, O., 2012. The stability of grounding lines on retrograde slopes. The Cryosphere Discussions 6, 2597–2619.

Healey, M., 2011. The cumulative impacts of climate change on Fraser River sockeye salmon (Oncorhynchus nerka) and implications for management. Can. J. Fish. Aquat. Sci. 68, 718–737. https://doi.org/10.1139/f2011-010

Hiebert, J., Cannon, A., Murdock, T., Sobie, S., Werner, A., 2018. ClimDown: Climate Downscaling in R, Journal of Open Source Software. https://doi.org/10.21105/joss.00360

Hinch, S.G., Martins, E.G., 2011. A review of potential climate change effects on survival of Fraser River sockeye salmon and an analysis of interannual trends in en route loss and pre-spawn mortality (Cohen Commission Technical Report No. 9), The Cohen Commission of Inquiry into the Decline of Sockeye Salmon in the Fraser River. Vancouver, BC.

Hunter, K.L., Wade, J., Stortini, C.H., Hyatt, K.D., Christian, J.R., Pepin, P., Pearsall, I.A., Nelson, M.W., Perry, R.I., Shackell, N.L., 2015. Climate Change Vulnerability Assessment Methodology Workshop Proceedings (Canadian Manuscript Report of Fisheries and Aquatic Sciences No. 3086). Fisheries and Oceans Canada, Nanaimo, BC.

Hunter, R.D., Meentemeyer, R.K., 2005. Climatologically Aided Mapping of Daily Precipitation and Temperature. J. Appl. Meteor. 44, 1501–1510. https://doi.org/10.1175/JAM2295.1

Hyatt, Kim D., Alexander, C.A.D., Stockwell, M.M., 2015. A decision support system for improving “fish friendly” flow compliance in the regulated Okanagan Lake and River System of British Columbia. Canadian Water Resources Journal / Revue canadienne des ressources hydriques 40, 87–110. https://doi.org/10.1080/07011784.2014.985510

Hyatt, K.D., Stiff, H.W., Stockwell, M.M., Leudke, W., D.P. Rankin, Dobson, D., Till, J., 2015. A Synthesis of Adult Sockeye Salmon Migration and Environmental Observations for the Somass Watershed, 1974-2012 (Canadian Manuscript Report of Fisheries and Aquatic Sciences No. 3115). Fisheries and Oceans Canada, Science Branch, Pacific Region, Pacific Biological Station, Nanaimo, British Columbia.

Hyatt, K.D., Stockwell, M.M., Rankin, D.P., 2003. Impact and Adaptation Responses of Okanagan River Sockeye Salmon (Oncorhynchus nerka) to Climate Variation and Change Effects During Freshwater Migration: Stock Restoration and Fisheries Management Implications. Canadian Water Resources Journal / Revue canadienne des ressources hydriques 28, 689–713. https://doi.org/10.4296/cwrj2804689

IPCC, 2021. Summary for Policymakers, in: V. Masson-Delmotte, P. Zhai, A. Pirani, S.L. Connors, C. Péan, S. Berger, N. Caud, Y. Chen, L. Goldfarb, M.I. Gomis, M. Huang, K. Leitzell, E. Lonnoy, J.B.R. Matthews, T.K. Maycock, T. Waterfield, O. Yelekçi, R. Yu, B. Zhou (Eds.), Climate Change 2021: The Physical Science Basis. Contribution of Working Group I to the Sixth Assessment Report of the Intergovernmental Panel on Climate Change. Cambridge University Press, Canbridge, United Kingdom and New York, NY, USA, pp. 3–32. https://doi.org/10.1017/9781009157896.001

IPCC, 2014. Climate Change 2014: Impacts, Adaptation, and Vulnerability. Part A: Global and Sectoral Aspects. Contribution of Working Group II to the Fifth Assessment Report to the Intergovernmental Panel on Climate Change. Cambridge University Press, Cambridge, UK, and New York, NY, USA.

Isaak, D.J., Wollrab, S., Horan, D., Chandler, G., 2012. Climate change effects on stream and river temperatures across the northwest U.S. from 1980–2009 and implications for salmonid fishes. Climatic Change 113, 499–524. https://doi.org/10.1007/s10584-011-0326-z

Knighton, D., 1998. Fluvial Forms and Processes. Arnold, London.

Levy, D., Woodey, J., Hardy, L., 2007. Stuart Area Sockeye Salmon Runs and their Importance to the First Nations of the Upper Fraser River Watershed. Upper Fraser Fisheries Conservation Alliance, Prince George, B.C.

Liang, X., Lettenmaier, D.P., Wood, E.F., Burges, S.J., 1994. A simple hydrologically based model of land-surface water and energy fluxes for general-circulation models. Journal of Geophysical Research-Atmospheres 99, 14415–14428. https://doi.org/10.1029/94JD00483

Liang, X., Wood, E.F., Lettenmaier, D.P., 1996. Surface soil moisture parameterization of the VIC-2L model: Evaluation and modification. Global and Planetary Change, Soil Moisture Simulation 13, 195–206. https://doi.org/10.1016/0921-8181(95)00046-1

Macdonald, J.S., Morrison, J., Patterson, D.A., 2012. The Efficacy of Reservoir Flow Regulation for Cooling Migration Temperature for Sockeye Salmon in the Nechako River Watershed of British Columbia. North American Journal of Fisheries Management 32, 415–427. https://doi.org/10.1080/02755947.2012.675946

Mantua, N., Tohver, I., Hamlet, A., 2010. Climate change impacts on streamflow extremes and summertime stream temperature and their possible consequences for freshwater salmon habitat in Washington State. Climatic Change 102, 187–223. https://doi.org/Article

Marsha, A.L., Steel, E.A., Fullerton, A.H., 2021. Modeling thermal metrics of importance for native vs non-native fish across stream networks to provide insight for watershed-scale fisheries management. Freshwater Science 40, 120–137. https://doi.org/10.1086/713038

Martins, E.G., Hinch, S.G., Patterson, D.A., Hague, M.J., Cooke, S.J., Miller, K.M., Lapointe, M.F., English, K.K., Farrell, A.P., 2011. Effects of river temperature and climate warming on stock-specific survival of adult migrating Fraser River sockeye salmon (Oncorhynchus nerka). Global Change Biology 17, 99–114. https://doi.org/10.1111/j.1365-2486.2010.02241.x

Maurer, E.P., Hidalgo, H.G., Das, T., Dettinger, M.D., Cayan, D.R., 2010. The utility of daily large-scale climate data in the assessment of climate change impacts on daily streamflow in California. Hydrol. Earth Syst. Sci. 14, 1125–1138. https://doi.org/10.5194/hess-14-1125-2010

Mayer, N.B., Hinch, S.G., Eliason, E.J., 2024. Thermal tolerance in Pacific salmon: A systematic review of species, populations, life stages and methodologies. Fish and Fisheries 25, 283–302. https://doi.org/10.1111/faf.12808

McDaniels, T., Wilmot, S., Healey, M., Hinch, S., 2010. Vulnerability of Fraser River sockeye salmon to climate change: A life cycle perspective using expert judgments. Journal of Environmental Management 91, 2771–2780. https://doi.org/10.1016/j.jenvman.2010.08.004

Ministry of Forests, 2024. Freshwater Atlas - Province of British Columbia [WWW Document]. URL https://www2.gov.bc.ca/gov/content/data/geographic-data-services/topographic-data/freshwater (accessed 4.11.24).

Mohseni, O., Stefan, H.G., Erickson, T.R., 1998. A nonlinear regression model for weekly stream temperatures. Water Resources Research 34, 2685–2692. https://doi.org/10.1029/98WR01877

Morrison, J., Foreman, M.G.G., 2005. Forecasting Fraser River flows and temperatures during upstream salmon migration. Journal of Environmental Engineering & Science 4, 101–111. https://doi.org/10.1139/S04-046

Morrison, J., Quick, M.C., Foreman, M.G.G., 2002. Climate change in the Fraser River watershed: flow and temperature projections. Journal of Hydrology 263, 230–244. https://doi.org/10.1016/S0022-1694(02)00065-3

Natural Resources Canada/ The Canada Centre for Mapping and Earth Observation (NRCan/CCMEO), United States Geological Survey (USGS), Insituto Nacional de Estadística y Geografía (INEGI), Comisión Nacional para el Conocimiento y Uso de la Biodiversidad (CONABIO), and Comisión Nacional Forestal (CONAFOR), 2013. 2013: 2010 North American Land Cover at 250 m spatial resolution.

Parmesan, C., Morecroft, M.D., Trisurat, Y., Adrian, R., Anshari, G.Z., Arneth, A., Gao, Q., Gonzalez, P., Harris, R., Price, J., Stevens, N., Talukdarr, G.H., 2022. Terrestrial and Freshwater Ecosystems and their Services, in: Pörtner, H.-O., Roberts, D.C., Tignor, M., Poloczanska, E.S., Mintenbeck, K., Alegría, A., Craig, M., Langsdorf, S., Löschke, S., Möller, V., Okem, A., Rama, B. (Eds.), Climate Change 2022: Impacts, Adaptation, and Vulnerability. Contribution of Working Group II to the Sixth Assessment Report of the Intergovernmental Panel on Climate Change. Cambridge University Press.

Peterman, R.M., Dorner, B., 2012. A widespread decrease in productivity of sockeye salmon (Oncorhynchus nerka) populations in western North America. Can. J. Fish. Aquat. Sci. 69, 1255–1260. https://doi.org/10.1139/f2012-063

Pfeffer, W.T., Arendt, A.A., Bliss, A., Bolch, T., Cogley, J.G., Gardner, A.S., Hagen, J.-O., Hock, R., Kaser, G., Kienholz, C., Miles, E.S., Moholdt, G., Mölg, N., Paul, F., Radić, V., Rastner, P., Raup, B.H., Rich, J., Sharp, M.J., Consortium, T.R., 2014. The Randolph Glacier Inventory: a globally complete inventory of glaciers. Journal of Glaciology 60, 537–552. https://doi.org/10.3189/2014JoG13J176

Piotrowski, A.P., Zhu, S., Napiorkowski, J.J., 2022. Air2water model with nine parameters for lake surface temperature assessment. Limnologica 94, 125967. https://doi.org/10.1016/j.limno.2022.125967

Quick, M.C., Pipes, A., 1977. U.B.C. WATERSHED MODEL / Le modèle du bassin versant U.C.B. Hydrological Sciences Bulletin 22, 153–161. https://doi.org/10.1080/02626667709491701

Quinn, T.P., Hodgson, S., Peven, C., 1997. Temperature, flow, and the migration of adult sockeye salmon (Oncorhynchus nerka) in the Columbia River. Canadian Journal of Fisheries and Aquatic Sciences 54, 1349–1360. https://doi.org/10.1139/f97-038

Richter, A., Kolmes, S.A., 2005. Maximum Temperature Limits for Chinook, Coho, and Chum Salmon, and Steelhead Trout in the Pacific Northwest. Reviews in Fisheries Science 13, 23–49. https://doi.org/10.1080/10641260590885861

Salinger, D.H., Anderson, J.J., 2006. Effects of Water Temperature and Flow on Adult Salmon Migration Swim Speed and Delay. Transactions of the American Fisheries Society 135, 188–199. https://doi.org/10.1577/t04-181.1

Schnorbus, M., 2018. VIC Glacier: Description of VIC model changes and updates (PCIC Internal Report). Pacific Climate Impacts Consortium, Victoria, BC.

Schnorbus, M.A., 2024. VIC-GL - DynWat Model Deployment. Pacific Climate Impacts Consortium, Victoria, B.C.

Schoeneberg, A.T., Larabi, S., Schnorbus, M., 2023. Raven Model Deployment Report. BC Salmon Restoration and Innovation Fund Project Number BCSRIF-2019-074-2 (BC Salmon Restoration and Innovation Fund Project Number BCSRIF-2019-074-2). Pacific Climate Impacts Consortium, Victoria, B.C.

Schwarzwald, K., Lenssen, N., 2022. The importance of internal climate variability in climate impact projections. Proceedings of the National Academy of Sciences 119, e2208095119. https://doi.org/10.1073/pnas.2208095119

Shanley, C.S., Albert, D.M., 2014. Climate Change Sensitivity Index for Pacific Salmon Habitat in Southeast Alaska. PLOS ONE 9, e104799. https://doi.org/10.1371/journal.pone.0104799

Simard, M., Pinto, N., Fisher, J.B., Baccini, A., 2011. Mapping forest canopy height globally with spaceborne lidar. Journal of Geophysical Research: Biogeosciences 116. https://doi.org/10.1029/2011JG001708

Sobie, S.R., Murdock, T.Q., 2017. High-Resolution Statistical Downscaling in Southwestern British Columbia. Journal of Applied Meteorology and Climatology 56, 1625–1641. https://doi.org/10.1175/JAMC-D-16-0287.1

Stiff, H.W., Hyatt, K.D., Cone, T.E., Patterson, D.A., Benner, K., 2018a. Water temperature, river discharge, and adult Sockeye salmon migration observations in the Quesnel/Horsefly watershed (Canadian

Manuscript Report of Fisheries and Aquatic Sciences No. 3154). Fisheries and Oceans Canada, Nanaimo, BC.
Stiff, H.W., Hyatt, K.D., Hall, P., Finnegan, B., Macintyre, D., 2015a. Water Temperature, River Discharge, and Adult Sockeye Salmon Migration Observations in the Babine Watershed, 1946-2014 (Canadian Manuscript Report of Fisheries and Aquatic Sciences No. 3053). Fisheries and Oceans Canada, Nanaimo, BC.
Stiff, H.W., Hyatt, K.D., Patterson, D.A., Benner, K., Cone, T.E., Grinder, P., Billyboy, R., 2017. Water temperature, river discharge, and adult Sockeye salmon migration observations in the Chilko-Chilcotin watershed, 1975-2012 (Canadian Manuscript Report of Fisheries and Aquatic Sciences No. 3114). Fisheries and Oceans Canada, Nanaimo, BC.
Stiff, H.W., Hyatt, K.D., Stockwell, M.M., Cannon, A.J., 2018b. Downscaled GCM trends in projected air and water temperature to 2100 due to climate variation in six sockeye salmon watersheds (Canadian Technical Report of Fisheries and Aquatic Sciences No. 3259). Fisheries and Oceans Canada, Nanaimo, BC.
Stiff, H.W., Hyatt, K.D., Stockwell, M.M., Cox-Rogers, S., Hall, P., Alexander, R., Kingshott, S.C., Percival, N., Stewart, B., 2015b. Water Temperature, River Discharge, and Adult Sockeye Salmon Migration Observations in the Meziadin Watershed, 1966-2012 (Canadian Manuscript Report of Fisheries and Aquatic Sciences No. 3019). Fisheries and Oceans Canada, Nanaimo, BC.
Stiff, H.W., Hyatt, K.D., Stockwell, M.M., Etherton, P.M., Waugh, W.D., 2013. Water temperature, river discharge, and adult Sockeye salmon migration observations for the Tahltan watershed, 1959-2012 (Canadian Manuscript Report of Fisheries and Aquatic Sciences No. 3018). Fisheries and Oceans Canada, Nanaimo, BC.
Stiff, H.W., Hyatt, K.D., Vulstek, S.C., Russell, J.R., Joyce, J.E., 2019. Water temperature, water level, and adult Sockeye salmon migration observations in Auke Creek, Alaska (Canadian Manuscript Report of Fisheries and Aquatic Sciences No. draft). Fisheries and Oceans Canada, Nanaimo, BC.
Sykes, G.E., Johnson, C.J., Shrimpton, J.M., 2009. Temperature and Flow Effects on Migration Timing of Chinook Salmon Smolts. Transactions of the American Fisheries Society 138, 1252–1265. https://doi.org/10.1577/t08-180.1
Taylor, K.E., Stouffer, R.J., Meehl, G.A., 2012. An Overview of CMIP5 and the Experiment Design. Bulletin of the American Meteorological Society 93, 485–498. https://doi.org/10.1175/BAMS-D-11-00094.1
Todini, E., 1996. The ARNO rainfall—runoff model. Journal of Hydrology 175, 339–382. https://doi.org/10.1016/S0022-1694(96)80016-3
Toffolon, M., Piccolroaz, S., 2015. A hybrid model for river water temperature as a function of air temperature and discharge. Environmental Research Letters 10, 114011. https://doi.org/10.1088/1748-9326/10/11/114011
Tsuruta, K., Schnorbus, M.A., 2022. Assessing the influence of calibration methodology and model structure on glacio-hydrological simulations in the Cheakamus River Basin, British Columbia, Canada. Journal of Hydrology X 17, 100144. https://doi.org/10.1016/j.hydroa.2022.100144
Tsuruta, K., Schnorbus, M.A., 2021. Exploring the operational impacts of climate change and glacier loss in the upper Columbia River Basin, Canada. Hydrological Processes 35, e14253. https://doi.org/10.1002/hyp.14253
van Beek, L.P.H., Eikelboom, T., van Vliet, M.T.H., Bierkens, M.F.P., 2012. A physically based model of global freshwater surface temperature. Water Resources Research 48. https://doi.org/10.1029/2012WR011819
van Vuuren, D.P., Edmonds, J., Kainuma, M., Riahi, K., Thomson, A., Hibbard, K., Hurtt, G.C., Kram, T., Krey, V., Lamarque, J.-F., Masui, T., Meinshausen, M., Nakicenovic, N., Smith, S.J., Rose, S.K.,

2011. The representative concentration pathways: an overview. Climatic Change 109, 5–31. https://doi.org/10.1007/s10584-011-0148-z

Wade, A.A., Beechie, T.J., Fleishman, E., Mantua, N.J., Wu, H., Kimball, J.S., Stoms, D.M., Stanford, J.A., 2013. Steelhead vulnerability to climate change in the Pacific Northwest. Journal of Applied Ecology 50, 1093–1104. https://doi.org/10.1111/1365-2664.12137

Wainwright, T.C., Weitkamp, L.A., 2013. Effects of climate change on oregon coast coho salmon: Habitat and life-cycle interactions. Northwest Science 87, 219–242. https://doi.org/10.3955/046.087.0305

Wanders, N., van Vliet, M.T.H., Wada, Y., Bierkens, M.F.P., van Beek, L.P.H. (Rens), 2019. High-Resolution Global Water Temperature Modeling. Water Resources Research 55, 2760–2778. https://doi.org/10.1029/2018WR023250

Waples, R.S., Gustafson, R.G., Weitkamp, L.A., Myers, J.M., Jjohnson, O.W., Busby, P.J., Hard, J.J., Bryant, G.J., Waknitz, F.W., Nelly, K., Teel, D., Grant, W.S., Winans, G.A., Phelps, S., Marshall, A., Baker, B.M., 2001. Characterizing diversity in salmon from the Pacific Northwest. Journal of Fish Biology 59, 1–41. https://doi.org/10.1111/j.1095-8649.2001.tb01376.x

Werner, A.T., Cannon, A.J., 2016. Hydrologic extremes – an intercomparison of multiple gridded statistical downscaling methods. Hydrology and Earth System Sciences 20, 1483–1508. https://doi.org/10.5194/hess-20-1483-2016

Werner, A.T., Schnorbus, M.A., Shrestha, R.R., Cannon, A.J., Zwiers, F.W., Dayon, G., Anslow, F., 2019. A long-term, temporally consistent, gridded daily meteorological dataset for northwestern North America. Scientific Data 6, 180299. https://doi.org/10.1038/sdata.2018.299

WSAC, 2019. Recommendations for a Made-in-B.C. Wild Salmon Strategy. B.C. Wild Salmon Advisory Council.

Wu, H., Kimball, J.S., Li, H., Huang, M., Leung, L.R., Adler, R.F., 2012. A new global river network database for macroscale hydrologic modeling. Water Resources Research 48. https://doi.org/10.1029/2012WR012313